

COALESCED DELTA-FRONT SHEET-LIKE SANDSTONE BODIES FROM HIGHLY AVULSIVE DISTRIBUTARY CHANNELS: THE LOW-ACCOMMODATION MESA RICA SANDSTONE (DAKOTA GROUP, NEW MEXICO, U.S.A.)

ANNA E. VAN YPEREN,¹ JOHN M. HOLBROOK,² MIQUEL POYATOS-MORÉ,¹ AND IVAR MIDTKANDAL¹

¹*Department of Geosciences, University of Oslo, 0316 Oslo, Norway*

²*Department of Geological Sciences, Texas Christian University, Fort Worth, Texas 76129, U.S.A.*
e-mail: annavanyperen@gmail.com

ABSTRACT: Low-accommodation deltaic systems are often challenging to interpret due to their condensed, low-gradient nature, which often results in extensive, sheet-like sandstone bodies. As a result, detailed studies of such systems are scarce, and their internal depositional architecture is still poorly understood. We analyze one such system, the Cenomanian deltaic Mesa Rica Sandstone (Dakota Group), which was deposited in the Western Interior Seaway, in east-central New Mexico, USA. A > 20-km-long escarpment, subparallel to the main delta progradation direction, allows a detailed analysis of facies distribution, depositional architecture, and the spatial extent of stratigraphic surfaces. Results reveal an arrangement of laterally variable shallowing-upward facies successions with three depositional cycles preserved. The first cycle is characterized by deltaic sheet-like sandstone bodies that are consistently overlain by sand-filled amalgamated distributary-channel deposits. The two successive cycles record a progressive reduction of sediment supply into the basin. Vertical and lateral relationships between facies associations and architectural geometries allow the recognition of regional key stratal surfaces, incised-valley fills, and the presence of lagoonal deposits at a sub-regional scale.

The Mesa Rica deltaic system represents a river-dominated delta with multiple distributary channels. The sheet-like delta-front sandstone bodies are interpreted as the result of the combined effect of high sandy-sediment supply and low accommodation. The latter acted as an accelerator for autogenic depositional mechanisms such as mouth-bar deposition and abandonment, and for the highly avulsive character of distributary channels. After deposition, minor wave reworking facilitated lateral sand redistribution and favored bioturbation. This study demonstrates that sheet-like delta-front sandstone geometries from low-accommodation systems can be formed without the dominance of wave redistribution processes. This cautions against interpretations of amalgamated shoreline systems based solely on apparent sandstone geometries, without taking into account the preservation potential and postdepositional modification of primary deltaic characteristics.

INTRODUCTION

The large-scale architecture of ancient deltaic systems has been extensively documented by stratigraphic (e.g., Galloway 1975; Willis et al. 1999; Gani and Bhattacharya 2005) and sequence stratigraphic studies (e.g., Bhattacharya and Walker 1991; Martinsen 1993; Plint 2000; Garrison and Van den Bergh 2004). However, deltaic architecture is highly dependent on available accommodation. Facies distribution and stacking patterns show major contrasts between high- and low-accommodation deltaic systems (e.g., Ainsworth et al. 2017). Although low-accommodation deltas have received recent attention (e.g., Olariu et al. 2005; Fielding et al. 2006; Allen and Fielding 2007; Gani and Bhattacharya 2007; Fielding et al. 2009; Antia and Fielding 2011; Di Celma et al. 2016; Ainsworth et al. 2017), they are still underrepresented in the literature.

Low-accommodation systems are often characterized by relatively thin, condensed, and top-truncated units (e.g., Fielding et al. 2005; Antia and Fielding 2011), with predominantly lateral offset stacking and low

preservation potential of coeval delta-plain deposits (Gani and Bhattacharya 2007; Ainsworth et al. 2017). These low-gradient settings typically result in lobate sand bodies because of the frequent recurrence of bifurcation and avulsion processes, and thereby lateral sediment dispersal, from multiple successive entry points (Olariu and Bhattacharya 2006). The resulting facies architecture is different from that of elongate deltas, and can form laterally extensive shorelines and sand-body geometries similar to those of pure wave-dominated environments (Olariu and Bhattacharya 2006). In a variety of depositional environments, these laterally extensive deposits are often described as “sheet-like sandstones” (e.g., Potter 1967; Friend et al. 1979; Miall 1988; Winn 1991; Normark et al. 1993; Walker and Bergman 1993; Bhattacharya and Giosan 2003). This term applies to the overall geometry, and such sandstone bodies can show considerable variability in internal structure (e.g., Potter 1967; Miall 1988).

Sequence stratigraphic models often invoke allogenic variations in relative sea level as key controls on stratal architecture (e.g., Posamentier and Vail 1988; Galloway 1989; Bhattacharya and Willis 2001; Neal and Abreu 2009; Hampson 2016), with the ratio of accommodation to sediment

supply (A:S) as the key descriptor for deltaic shoreline behavior (e.g., Olariu 2014). However, other controls such as internal autogenic dynamics of sediment routing systems and nearshore along-strike variability are also important (Olariu 2014; Hampson 2016; Madof et al. 2016), resulting in a nonlinear relationship between accommodation and sediment supply (e.g., Martinsen and Helland-Hansen 1995; Muto and Steel 1997; Olariu 2014; Madof et al. 2016). At delta-lobe and mouth-bar scale, the competition between waves, tides, and river discharge is a first-order control on depositional geometries (e.g., Wright and Coleman 1973; Jerolmack and Swenson 2007; Geleynse et al. 2011; Anthony 2015). Low-accommodation settings create additional challenges to distinguish between the preserved signal of allogenic and/or autogenic mechanisms. In addition, low-accommodation settings can accelerate autogenic processes such as channel avulsion and bifurcation, and the formation, migration, and eventual abandonment of mouth bars (e.g., Bryant et al. 1995; Olariu and Bhattacharya 2006; Edmonds and Slingerland 2007).

The influence of basin water depth on delta morphology has been addressed by flume-tank and modeling studies, which show that deep-basin deltas have fewer channels than shallow-basin deltas (Storms et al. 2007; Liang et al. 2015), and are characterized by less frequent channel migration and avulsion (Muto et al. 2016). Results of analog modeling from Bijkerk et al. (2016) demonstrate that progradation in low-accommodation settings leads to inefficient sediment transport and more deposition on the coastal plain. These results contradict many stratigraphic models in which low accommodation is interpreted to promote sediment bypass (e.g., Posamentier et al. 1988; Emery and Myers 2009).

Despite significant recent progress towards documenting and understanding deltaic development in low-accommodation settings, uncertainties remain concerning depositional mechanisms and resulting stratigraphic architectures. The fluvial to deltaic Mesa Rica Sandstone, which was deposited in the Western Interior Seaway, provides a rare opportunity to reconstruct the development of a low-accommodation delta, although there has been little detailed analysis of its facies architecture, lateral and vertical changes, and stratigraphic development (e.g., Kisucky and Wright 1986; Kisucky 1987; Holbrook and Dunbar 1992; Scott et al. 2004). The objectives for this paper are: i) to describe and analyze the spatial distribution of sedimentary facies, architectural elements, and key stratal surfaces; ii) to utilize the established stratigraphic framework to reconstruct the paleogeographic evolution of the system; and iii) to generate a conceptual model for the development of coalesced delta-front sheet-like sandstone bodies.

GEOLOGICAL SETTING

The Mesa Rica Sandstone (hereinafter referred to as “Mesa Rica”) was deposited during the Cenomanian in the Cordilleran foreland basin (Fig. 1A), and is the oldest formation in the Dakota Group in Colorado and New Mexico (e.g., Holbrook and Dunbar 1992; Scott et al. 2004; Scott et al. 2018). Subduction of the Farallon plate beneath the west coast of North America caused back-arc compression in the Late Jurassic, initiating the Cordilleran orogeny (DeCelles 2004). The resultant Sevier fold-and-thrust belt sourced eastward-prograding sedimentary systems of the US Western Interior, including the Dakota Group. A provenance study (MacKenzie and Poole 1962) supports a sediment source from pre-Cretaceous sedimentary rocks of the Cordilleran region. The Dakota Group also received minor sediment volumes from smaller topographic highs (Kisucky 1987; Holbrook and Dunbar 1992). The contemporaneous Mesa Rica delta was deposited in the Tucumcari Basin, in east-central New Mexico, which formed during the late Carboniferous and early Permian as a tectonic element of the Ancestral Rocky Mountains (Broadhead 2004). During the Cretaceous, the study area was located at $\sim 35^\circ\text{N}$ latitude, with a prevailing warm and humid climate (Chumakov et al. 1995).

The Dakota Group extends throughout the US Western Interior and is younger from east to west Colorado (e.g., Antia and Fielding 2011) (Fig. 1B). An overall NNW (proximal) to SSE (distal) depositional orientation characterizes the Dakota Group sandstone and shale succession in Colorado and northeast New Mexico. Here, the Dakota Group is further subdivided into the Mesa Rica, Pajarito, and Romeroville Formations (Fig. 1B). Three depositional transgression–regression cycles are identified, recording high-frequency relative sea-level fluctuations. These cycles are defined by regionally recognized sequence stratigraphic surfaces (e.g., Holbrook and Dunbar 1992; Holbrook 1996; Scott et al. 2004; Oboh-Ikuenobe et al. 2008) (Fig. 1B), and have been variously linked to Milankovitch cyclicity (Scott et al. 1998; Miller et al. 2004; Ma et al. 2014; Eldrett et al. 2015) and regional tectonics (Bhattacharya and Willis 2001; Vakarelov et al. 2006). Regional sequence boundary SB3.1 (Fig. 1B) forms the base of the Mesa Rica and is related to late Albian–early Cenomanian regression that caused widespread erosion in southeast Colorado and northeast New Mexico (Holbrook and Dunbar 1992; Holbrook 1996, 2001; Scott et al. 2004; Oboh-Ikuenobe et al. 2008). The Tucumcari Shale which underlies the Mesa Rica, represents a fully open marine environment (Scott 1970; Kues and Lucas 2001; Scott et al. 2004; Oboh-Ikuenobe et al. 2008).

Estimates of minimum (2×10^{-6} m/km) to maximum (1×10^{-4} m/km) slope gradients for the fluvial Mesa Rica to coexisting deltaic system (Oboh-Ikuenobe et al. 2008) indicate a low-gradient depositional setting.

METHODS AND DATA

The study area is part of a NNE–SSW-trending escarpment that stretches for approximately 320 km from the northeast corner of the Texas Panhandle (Fig. 1A), and forms the western edge of the Llano Estacado high plains. Based on the paleocurrent data collected, the study area extends subparallel to the depositional dip direction for ~ 20 km, with ~ 1 km strike control provided by NW–SE-trending canyons (Fig. 2). The Bonita fault creates an outcrop-belt limit to the SE in the study area (Fig. 2), and has a throw of 150–200 m (Stearns 1972).

Thirty-one sections, measured at centimeter scale, document the main sedimentary characteristics and vertical facies relationships in the Tucumcari Shale, Mesa Rica Sandstone, and Pajarito Formation. Paleocurrent readings ($N = 215$) were measured from cross-stratification and current-ripple lamination. The average current directions were used to reconstruct values of real width from apparent widths of channel elements cropping out at various angles to the true cross-stream directions (e.g., Fabuel-Perez et al. 2009). Facies analysis is based on lithology, texture, and sedimentary structures, and ichnology and bioturbation intensity was recorded using the bioturbation index (BI) scheme of Taylor and Goldring (1993). We defined vertical stacking of facies associations and interpreted key sequence stratigraphic surfaces. Photomontages were combined with field sketches to document sedimentary body geometries, lateral distributions, and the extent of defined surfaces. These form the basis of a correlation panel constructed subparallel to the depositional dip, supplemented with a 1 km strike-oriented panel.

FACIES AND FACIES ASSOCIATIONS

Strata are divided into seventeen facies recognized based on observations of lithology, grain size, sedimentary structures, paleocurrents, trace fossils, and macrofossil content (Table 1, Figs. 3–5). These facies are grouped into eight facies associations (FA), reflecting different sedimentary environments (Table 2). Interpretations are based partly on lateral and vertical facies relationships (Fig. 6).

FA1: Prodelta

Description.—FA1 consists of dark gray to black fissile mudstone with varying silt content (facies 1) that commonly grades up into mudstone-

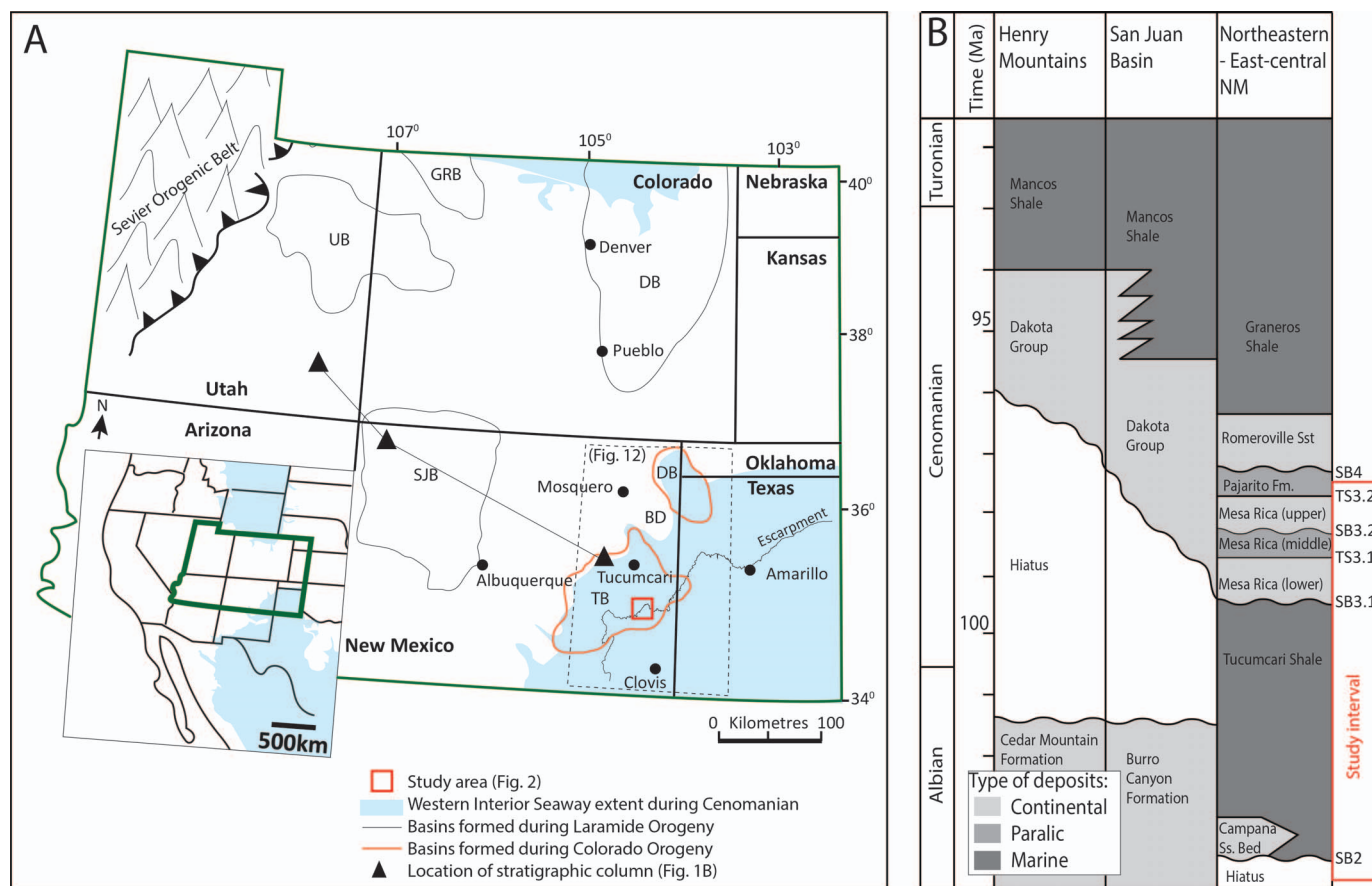


FIG. 1.—**A**) Map of the Western Interior during the Late Cretaceous (Cenomanian), including the approximate location of the Western Interior Seaway extent (light blue, Blakey 2014), and today's escarpment. Main basins that formed during Laramide Orogeny (black outline, Antia and Fielding 2011) and during Colorado Orogeny (orange outline, Suleimain and Keller 1985; Broadhead 2004) are indicated. **B**) Time-stratigraphic column for the Dakota Group and equivalent units from the Colorado Plateau (Henry Mountains and San Juan Basin; Antia and Fielding 2011) to northeastern–east-central New Mexico (Scott et al. 2004). Time scale after Scott et al. (2018). GRB, Green River Basin; UB, Uinta Basin; DB (Colorado), Denver Basin; SJB, San Juan Basin, TB, Tucumcari Basin; DB (New Mexico), Dalhart Basin; BD, Bravo Dome; SB, sequence boundary; TS, transgressive surface.

dominated heterolithic facies (facies 2). FA1 unit thicknesses vary between 11 and 21 m, and a pebble lag (facies 16) is locally present at the bases of FA1 units. The mudstone reveals minor to no bioturbation and contains numerous bivalve taxa, such as abundant *Texigryphaea* and *Peilinia levicostata* (Fig. 5A), and less common *Protocardia texana* and *Ostrea marshii* (e.g., Kues and Lucas 2001). Locally, the mudstone is interbedded with bioturbated (BI 4–6) sandstone beds (10–20 cm) with bivalve fragments. The degree of abrasion and proportion of broken versus unbroken shell fragments decreases progressively in the upper sandstone beds. FA1 grades vertically into distal delta front deposits (FA2).

Interpretation.—This facies association records deposition of prodelta mud below fair-weather wave base. The mud was deposited by suspension fallout after transport into the basin by episodic hyperpycnal low-density turbidity currents (Abouelresh and Slatt 2011). The low to absent bioturbation in the mudstone is characteristic of prodelta environments that experience river-induced stresses (MacEachern et al. 2005). The sandstone beds are interpreted as storm deposits, which is supported by the high bioturbation index. Temporarily increased wave agitation favored faunal living conditions by optimizing the distribution of oxygen, salinity, and temperature (Gani et al. 2009). The *Scabrotrigonia*–*Turritella* community and the biostrome-forming macrofaunal *Texigryphaea*–*Peilinia* community reflect mid-shoreface and lower-shoreface environments,

respectively (Scott 1974). The thin basal conglomerate lags are interpreted to result from ravinement of the underlying strata and represent onset of Albian transgression (e.g., Scott 1970).

FA2 comprises two subsets:

FA2: Distal Delta Front

Description.—FA2 is predominantly sandy and coarsens upward from very fine sandstone with a silt component to a clean fine-grained sandstone (Fig. 6C). FA2 units are on average 4–6 m thick and overlie FA1 locally with a sharp base (Fig. 6A, C). FA2 grades upwards into proximal delta deposits (FA3) and in places laterally into prodelta deposits (FA1).

FA2.a—Poorly bioturbated sandstone: This facies association consists of thin to thick (5–40 cm) sandstone beds with cross-stratification, and asymmetrical (current) and symmetrical (wave) ripple lamination (facies 12, 13; Fig. 3D), and locally, loading and dewatering features. Wave ripples occur predominantly in the lower part of the FA2.a package and are overlain by cross-laminated strata with wave-ripple lamination cannibalizing the bedform tops. Current ripples are locally mud-draped. Low-angle cross-stratification with scattered subangular extrabasinal clasts (average diameter 0.5 cm) is rare. Bioturbation is low and non-uniform (BI 0–1), and the only observed trace fossil is *Ophiomorpha*, recorded at locations 2 and 6 (Fig. 2).

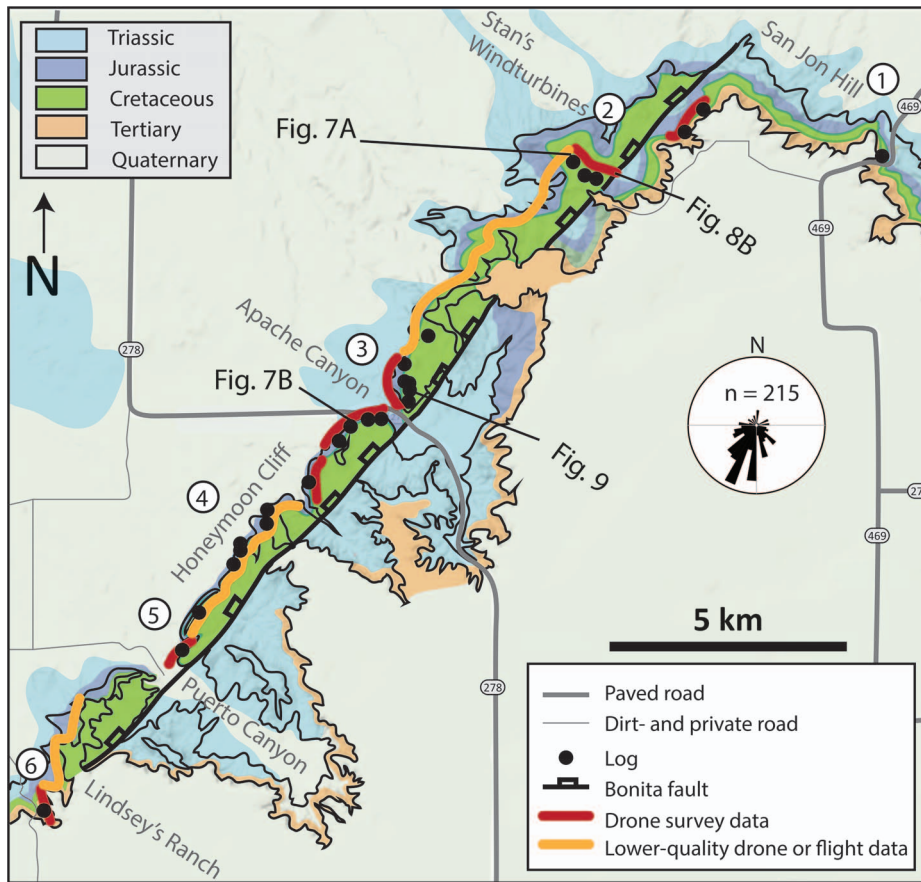


FIG. 2.—Map showing outcrop extent and dataset collected for the Mesa Rica Sandstone in the study area. Locations of the measured sections in Figure 7, correlation panels in Figure 8B, and photopanoramas in Figure 9. The complete paleocurrent data set ($N = 215$) as collected in this study demonstrates how the outcrop area extends along depositional dip direction. Location references used in text; San Jon Hill, location 1; Stan's Windturbines, location 2; Apache Canyon, location 3; Honeymoon Cliff, location 4; Puerto Canyon, location 5; Lindsey's Ranch, location 6.

FA2.b—Highly bioturbated sandstone: FA2.b is characterized by intense bioturbation (BI 5–6) which obliterates original bedding structures (facies 6; Fig. 5E). *Ophiomorpha*, *Thalassinoides*, *Cylindrichnus*, *Palaeophycus*, and less commonly *Skolithos* and *Rhizocorallium* are recognized, which together constitute the proximal *Cruziana* Ichnofacies (MacEachern and Bann 2008). The bioturbation index decreases towards the top of FA2.b. In the lower part of FA2.b, scattered clasts are common and ripple lamination is rare. In addition, very thin to medium (2–15 cm), normally graded, very fine- to fine-grained structureless micaceous sandstone beds with *Ophiomorpha* (BI 0–2) are common (facies 5; Fig. 3C). These beds have a vertical spacing of 30–80 cm. Thin beds tend to pinch out laterally, and medium beds commonly have sharp (in places erosional) bases, locally contain extrabasinal clasts, and display parallel lamination. Locally, FA2.b deposits stack in multiple (max. 4) coarsening-upward packages that are 1.5–2 m thick (Fig. 6A), and form extensive (almost tabular) sheet-like sedimentary bodies. Shells with a preferential concave-down orientation are locally abundant in the upper parts of the beds (Fig. 4B). In location 1 (Fig. 2), 10–60-cm-thick shellbeds reveal predominantly unbroken and tightly packed macrofauna which constitute the *Scabrotrigonia*–*Turritella* middle-shoreface faunal association (Scott 1974) (Fig. 5B).

Interpretation.—Distal deltaic deposits have two different expressions.

FA2.a: FA2.a represents deposits of an active river-dominated distal delta front with minor influences from wave and tidal energy (e.g., Coates and MacEachern 2009; Ainsworth et al. 2011). The low to absent bioturbation indicates a narrow colonization window. This is attributed to a nearby active distributary river mouth, which causes relatively high depositional rates, water turbidity, and fresh-water-induced stresses (MacEachern and Bann 2008; Gani et al. 2009). Minor wave influence is inferred from the presence

of symmetrical ripple lamination. Sporadic flaser bedding (mud-draped current-ripple foresets) may record tidal influence.

FA2.b: FA2.b records deposition in unstressed depositional conditions at the distal delta front. The high bioturbation intensities suggest a wide colonization window because of minimization of water turbidity and optimization of the distribution of oxygen, salinity, and temperature (MacEachern and Bann 2008; Gani et al. 2009). Increasing proximity to freshwater input is inferred from the characteristic upward-decreasing bioturbation trend (MacEachern and Bann 2008). The proximal *Cruziana* Ichnofacies corresponds to environments where energy levels shift from suspension-dominated to shifting substrate conditions (i.e., moderate energy) (MacEachern and Bann 2008). The thin normally graded fine-grained sandstone beds (facies 5) are interpreted as high-discharge event beds (or “hyperpycnites,” Mulder et al. 2003) from an extrabasinal river source. This sets them apart from conventional turbidites resulting from currents that originate within a basin (Zavala and Arcuri 2016).

FA3: Proximal Delta Front

Description.—FA3 (Fig. 5F) is composed of very fine- to fine-grained, and locally medium-grained, sandstone, with trough and tabular cross-bedding (facies 8, 9; Fig. 3A, B), parallel lamination (facies 10), a paucity of mudstone, and a low bioturbation index (BI 0–1). Trace fossils include *Skolithos* and *Ophiomorpha* (*Skolithos* Ichnofacies, MacEachern and Bann 2008). Sedimentary structures and bed boundaries are vaguely visible, and color grades from yellowish into grayish-white. Coal flakes are present in the uppermost beds. Paleocurrent data reveal a scattered pattern covering 360° variance, although SSW is the strongest component (Table 2). Convex-up lenticular geometries and accompanying onlapping surfaces (Fig. 6D, E) are definable locally.

TABLE 1.—Summary of facies in the Tucumcari Shale, Mesa Rica Sandstone, and Pajarito Formation in the study area. VF, very fine sand; F, fine sand; M, medium sand; VC, very coarse sand.

Lithology	Grain Size	Description	BI*	Biogenic Structures	Depositional Process
1 Black mudstone	Silty mud	Dark gray–black fissile mudstone with a varying silt content.	0–1	Macrofossils: <i>Texigryphaea</i> , <i>Peilinia levicostata</i> , <i>Protocardia texana</i> , <i>Ostrea marshii</i> Trace fossils: <i>unidentified</i>	Suspension fallout, low sedimentation rates.
2 Heterolithic, mud dominated	Mud–VF	Dark gray mudstone with densely distributed small-scale (1–6 mm) silt- to very fine-grained sandy lenses. The latter are in places unidirectional ripple-laminated.	3–4	Trace fossils: <i>Teichichnus</i> , <i>Thalassinoides</i> , <i>Phycosiphon</i> , <i>Siphonichnus</i> , <i>unidentified</i>	Alternating low energy with suspension fallout dominating. Sand is brought in by bioturbation from overlying sandy sediments or higher-energy episodes.
3 Heterolithic, equal proportions sand and mud	Mud–VF	Rippled sandstone lenses containing bidirectional and/or oscillation ripples.	0–3	Trace fossils: <i>unidentified</i>	Deposition in alternating energy with local tide influence.
4 Heterolithic, sand dominated	Mud–F	Structureless sandstone, rare plane parallel lamination, current ripples, and, more scarce, oscillation ripples. Local bidirectional current indicators and sediment loading. Some beds have floating granules and/or pebbles. Scarce single- and double-mud draped.	0–4	Trace fossils: <i>Rhizocorallium</i> , <i>Ophiomorpha</i> , <i>Planolites</i> , and <i>unidentified</i>	Deposition in alternating energy. Shallower than facies 3.
5 Structureless sandstone	VF–F	Erosional, sharp-based sandstones, completely structureless with normal grading. Grade into plane parallel-laminated intervals or irregular tops. Rare trough cross stratification. Common: scattered extrabasinal clasts (up to pebble size) in basal part, locally in medium grain-size matrix. When interbedded with facies 7, outstanding darker color. When in FA8, beds grade laterally into facies 12.	0–3	Macrofossils: <i>Texigryphaea</i> , <i>gastropods</i> , <i>unidentified</i> Trace fossils: <i>Ophiomorpha</i> , <i>Skolithos</i> , <i>Rhizolites</i>	Periodic high-energy discharge with variable flow intensities (bedload and suspended load). High sedimentation rates.
6 Shell bed	VF–F	10–60-cm-thick sandstone beds. Abundant but varying shell-content and variable but low amount of scattered clasts in sandstone beds. Bivalves are disarticulated but shells are often unbroken, tightly packed, and with no systematic orientation. Few beds consist of broken shell-fragments. Rare occurrence of calcareous sandstone beds with gastropods.	0–5	Macrofossils: <i>Texigryphaea</i> , <i>Peilinia levicostata</i> , <i>Protocardia texana</i> , <i>Turritella</i> , and <i>Sabrotrigonia</i> . Trace fossils: <i>Palaeophycus</i> , <i>Ophiomorpha</i> , <i>Skolithos</i> , <i>unidentified</i> .	Transported and disturbed-neighborhood assemblages. Beds with broken fragments are deposited during high-energy events.
7 Completely bioturbated sandstone	Si–F	Gradational based yellowish sandstone with completely obliterated primary sedimentary structures, silt laminae, and occasional scattered extrabasinal clasts (max 5 cm). Upward coarsening from silt to very fine sandstone into very fine to fine sandstone. Common: grades upwards into facies 10 and laterally into facies 1 and 2.	4–6	Macrofossils: <i>Texigryphaea</i> , <i>Peilinia levicostata</i> , <i>Protocardia texana</i> , <i>Turritella</i> Trace fossils: <i>Ophiomorpha</i> , <i>Skolithos</i> , <i>Thalassinoides</i> , <i>Rhizocorallium</i> , <i>Cylindrichnus</i> , <i>Palaeophycus</i> , <i>unidentified</i> horizontal trace fossils	High carrying capacity and bioturbation favorable conditions (optimized oxygen, salinity, temperature)
8 Trough cross-stratified sandstone	F–M	With and without clear bed boundaries. Less clear bed boundaries form a gradual continuation of underlying facies 7. Coal flakes can be present.	0–2	Trace fossils: <i>Skolithos</i> , <i>Ophiomorpha</i>	Migrating sinuous or linguoid dunes. Lower flow regime.
9 Cross-stratified sandstone	VF–M	Tabular bed boundaries, local lower erosional base. Commonly (dark) orange. Local inversely graded laminae. Dominantly planar and tangential tabular, very rare sigmoidal cross-stratification. Rare pebble-sized basal lag.	0–1	Bioturbated beds are very scarce. Trace fossils: <i>Skolithos</i> , <i>Ophiomorpha</i>	Migrating straight-crested or sinuous dunes with and without flow separation, lower flow regime.
10 Parallel-laminated sandstone	VF–F	White to light gray structureless or plane parallel. Rare low-angle cross-stratified sandstone.	0–3	Trace fossils: <i>Skolithos</i> , <i>rhizolites</i> ; mostly present in upper 70 cm	Upper-flow conditions, high sedimentation rates.
11 Disorganized sandstone	M	Structureless, ungraded sandstone with regularly distributed extrabasinal gravel (up to 1 cm) “floating” in medium-grained matrix.	0	Absent	Freezing of a sandy debris flow in base of channel/valley

TABLE 1.—Continued.

Lithology	Grain Size	Description	BI*	Biogenic Structures	Depositional Process
12 Asymmetrical ripple-laminated sandstone	Si-VF-F	Unidirectional current ripples. Occur as thick (< 1.2 m) (yellow-grayish) beds and at top of often structureless sandstone beds with thin silty mud in between.	0-2	Trace fossils: <i>Unidentified</i>	Migrating straight-crested ripples. Lower flow regime, low flow velocity.
13 Symmetrical ripple-laminated sandstone	Si-VF-F	Symmetrical ripples, often at tops of sandstone beds.	0-2	Trace fossils: <i>Unidentified</i>	Oscillatory flow above fairweather wave base.
14 Sandstone with undulatory bed boundaries	VF-F	Vari-colored sandstone beds with irregular bounding surfaces, often very thinly interbedded with silty mud. In places, beds show internal tangential cross stratification or plane parallel lamination.	0-2	Trace fossils: Low abundance, low diversity. <i>Skolithos</i> .	Irregular bounding surfaces could result from erosion of mud-draped bottomssets.
15 Back-flow ripples	VF-F	Superimposed small current ripples in direction opposite to their host bedform (facies 10).	0	Absent	Bedforms deposited by fluvial energy, modified by tides. Back-flow ripple formation due to lee-separation eddy flow under relatively high mean flow velocities.
16 Conglomerate	F-M matrix. Clasts VC to 7 cm	Erosional basal surface with extrabasinal clasts in a finer sandstone matrix. Clast-supported, subangular to subrounded. Grades into facies 9 or 10 and in places includes mud-silt rip-up clasts and/or wood debris. Alternatively, clasts are situated at the base of facies 1 or 2.	0	Absent	High-energy fluvial channel base. Or, when situated at the base of facies 1 or 2, transgressive lag formed by erosion and reworking.
17 Muddy siltstone	Mud-Si	Gray-brown muddy siltstone. Commonly vegetated.	0-1	Colored mottling is present at San Jon Hill (location 1).	Slow sedimentation from suspension fallout.

* BI = bioturbation index (Taylor and Goldring 1993)

Interpretation.—FA3 represents proximal delta-front deposits (Kisucky 1987). The widely scattered, low to almost absent bioturbation indicates high sedimentation rates, reduced salinity, and increased water turbidity, which is characteristic of river-dominated delta-front deposits (Gani et al. 2009). The random scatter of paleocurrent directions is evidence of unconfined, frequently changing flow at the channel mouth, with consequent lateral, downstream, and upstream growth of the mouth bar. Architectural elements that could be interpreted as terminal distributary channels (*sensu* Olariu and Bhattacharya 2006) were not observed. FA3 represents the proximal continuation of distal delta-front deposits (FA2), and is commonly abruptly succeeded vertically by distributary channel deposits (FA4).

FA4: Fluvial Distributary Channel

Description.—FA4 consists of fine- to medium-grained lensoid sandstone bodies bounded by erosional concave-upward surfaces, commonly lined with pebbles, wood, and muddy rip-up clasts (facies 16; Fig. 3F). Internally, these sandstone bodies are dominated by 15–40-cm-thick tabular (facies 9; Fig. 3A) and locally trough cross-beds (facies 8; Fig. 3B). The upper parts of these bodies locally display parallel- or ripple-laminated sandstone (facies 10, 12). Composite sandstone bodies have widths between 50 and 250 m and thicknesses that average 4–5 m (range 1–12 m). Cross-bedding orientations indicate unidirectional paleocurrents with a spread of ~120° and a mean direction of SSW (n = 145) (Table 2). Sandstone beds are devoid of bioturbation, mudstone drapes, or heterolithic bedding. Accretionary elements are rare.

Interpretation.—This facies association represents distributary-channel deposits. The prevalence of cross-stratification bounded by erosional concave-upward surfaces indicates deposition from 2D and 3D subaqueous dunes that migrated in response to relatively strong flows in confined channelized settings (e.g., Flemming 2000). The lack of bioturbation, mudstone drapes, or flaser bedding indicates an absence of marine influence. Holbrook (1996) measured average channel depths of 10–12 m and widths of 90–180 m for equivalent upstream Mesa Rica trunk channels. This implies that the smaller channel dimensions of FA4 might represent the result of successive downstream bifurcations from the trunk channel.

FA5: Beach Deposits

Description.—These strata are white to light gray, well-sorted sandstone deposits, mostly parallel laminated to low-angle (both N and S dips) parallel lamination, and with rare tabular cross-stratification (facies 9, 10). Locally, the tops of FA5 units display colored mottling, are bioturbated by roots or *Skolithos* (BI 0–3), and are commonly overlain by erosive channel-fill elements (FA4) (Fig. 5C). At location 1 (Fig. 2), NE-oriented foresets are up to a meter thick. FA5 is present most prominently in the proximal part of the study area (locations 1, 2; Fig. 2), and units of this FA become discontinuous in the down-dip direction (location 3; Fig. 2), where they overlie thin marine mudstone intervals. FA5 is absent in the distal part of the study area (locations 4, 5, 6; Fig. 2).

Interpretation.—FA5 records deposition in foreshore and backshore settings (Clifton et al. 1971). The northward-dipping low-angle parallel-laminated sandstone and local tabular cross-bedding may represent deposition in a backshore and/or washover-fan setting, respectively. The NE-oriented cross-lamination was created by dune migration in a paleo-landward direction and is interpreted as the result of beach-ridge migration. The southward-dipping low-angle parallel lamination dips paleo-seawards and is interpreted to represent foreshore deposition. Localized root

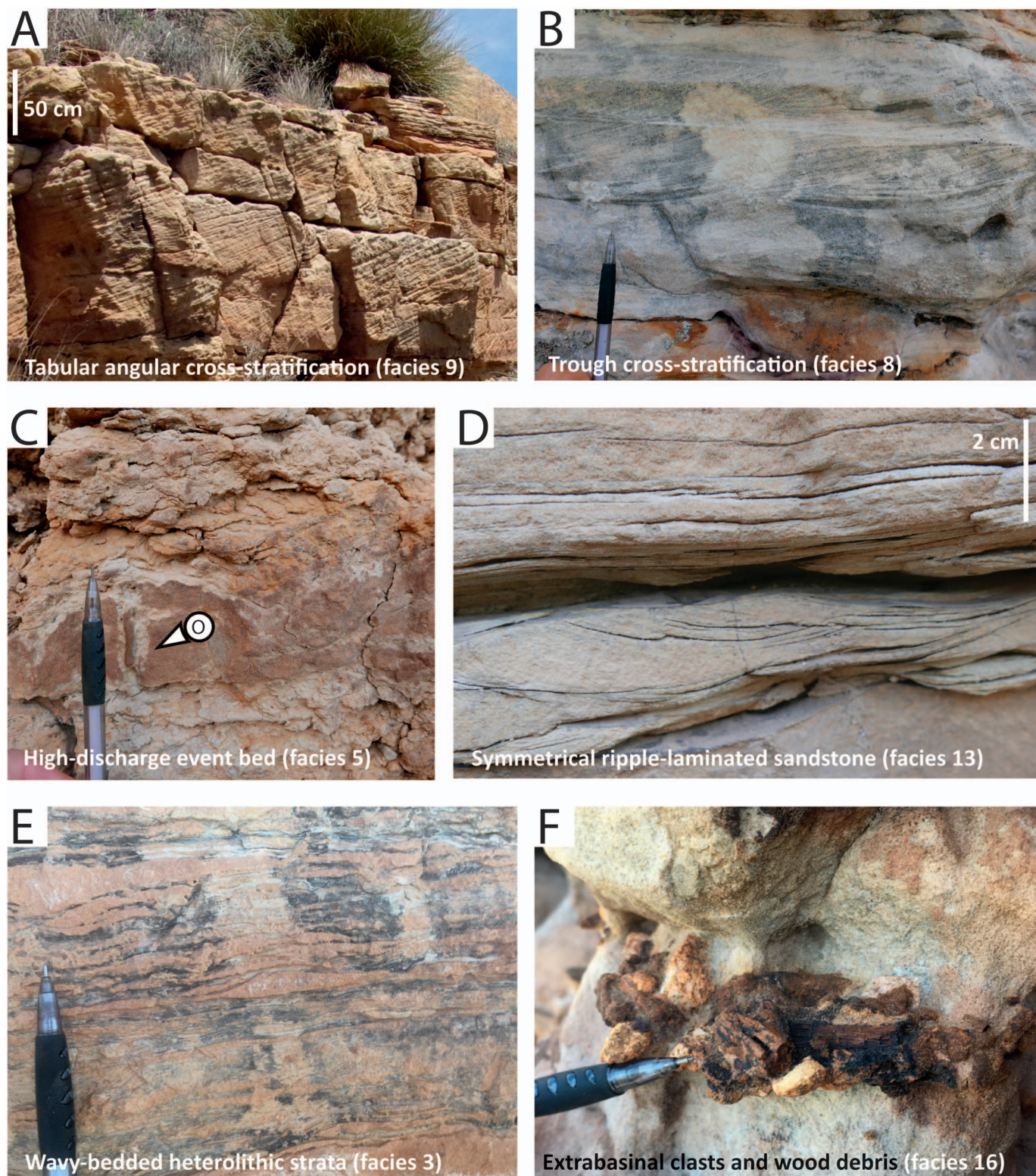


FIG. 3.—Photographs of selected facies (Table 1). **A**) Tabular angular cross-stratification (facies 9) in fluvial distributary channels (FA4). **B**) Trough cross-stratification (facies 8) in proximal delta-front sediments (FA3). **C**) High-discharge event bed (facies 5) interbedded with highly bioturbated (BI 5) sandstone beds (facies 7) in distal delta-front deposits (FA2.b) (*O. Ophiomorpha*). **D**) Symmetrical ripple-laminated sandstone (facies 13) in poorly bioturbated delta-front deposits (FA2.a). **E**) Wavy-bedded, heterolithic strata (facies 3) in lagoonal deposits (FA6). **F**) Wood debris and extrabasinal clasts (facies 16) lining the base of an erosional surface in fluvial distributary-channel deposits (FA4). 15-cm pencil for scale.

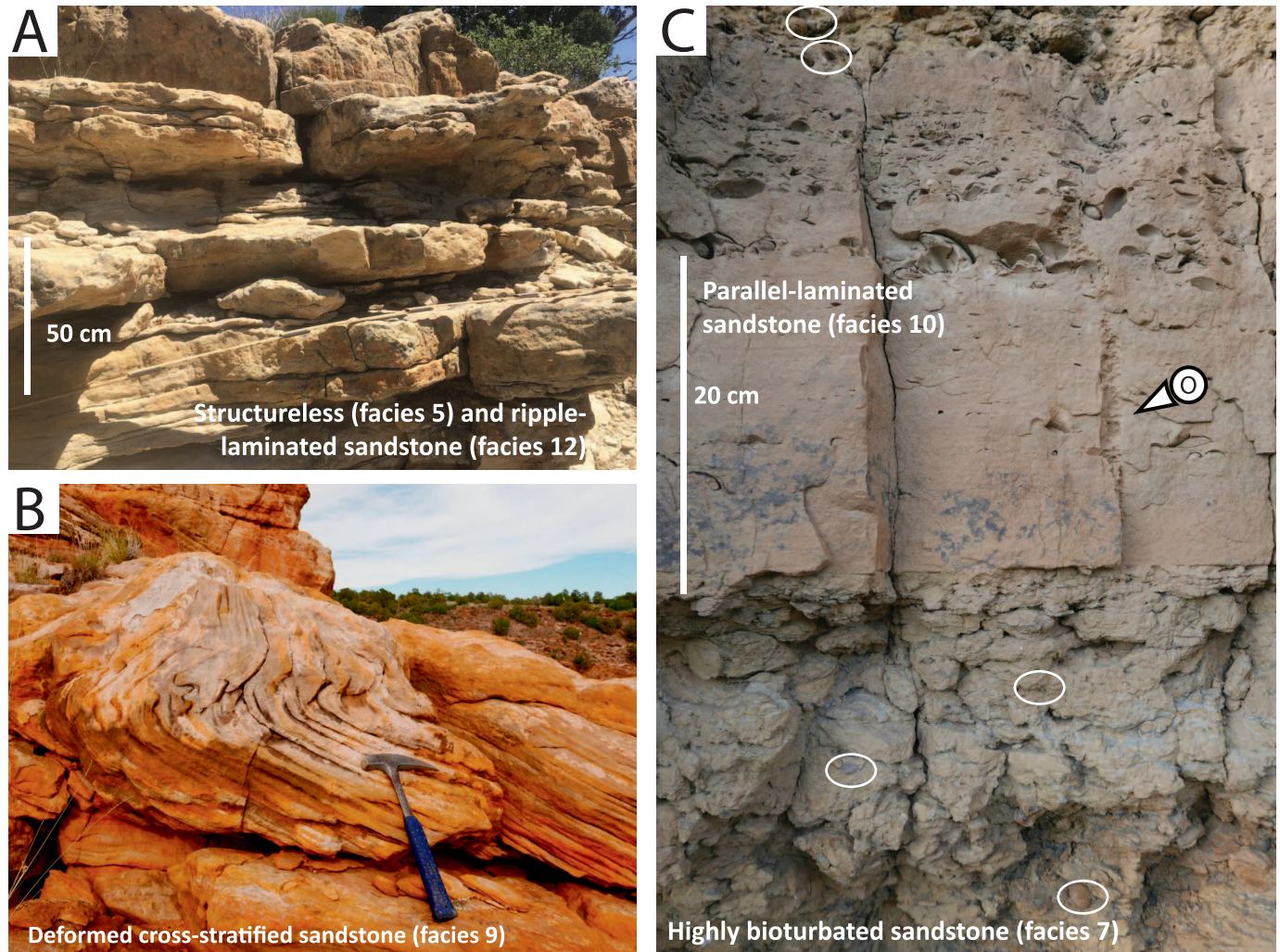


FIG. 4.—Photographs of selected facies (Table 1). **A**) Structureless sandstone beds with sharp bases and tops (facies 5) and ripple-laminated sandstone (facies 12), in lower-delta-plain-strata (FA8). **B**) Soft-sediment deformation in cross-stratified sandstone (facies 9), in fluvial distributary channels (FA4). **C**) Highly bioturbated (BI 5–6) very fine-grained sandstone (facies 7) interbedded with parallel-laminated fine-grained sandstone (facies 10), in distal delta-front sediments (FA 2.b), with scattered extrabasinal clasts (encircled). O, *Ophiomorpha*.

bioturbation represents weak pedogenesis related to periods of subaerial exposure.

FA6: Lagoon Deposits

Description.—This facies association is present only in the southernmost part of the study area (locations 5, 6; Fig. 2), and it displays a fining-upwards heterolithic succession consisting of flaser, wavy, and lenticular bedding with bidirectional paleocurrent indicators (facies 2, 3, 4) (Fig. 3E). Bioturbation is scarce to absent (BI 0–2) in the flaser and wavy bedding and includes *Ophiomorpha* and *Skolithos* (*Skolithos* Ichnofacies, MacEachern and Bann 2008). The sporadically bioturbated (BI 1–4) silty mudstone with lenticular bedding includes *Phycosiphon*, *Thalassinoides*, *Teichichnus*, and *Siphonichnus* (Fig. 5D). In the distal part of the study area (location 6; Fig. 2), this facies association is characterized by alternation of a) structureless fine-grained sandstone with rare preservation of roots, b) very fine sandstone, and c) muddy siltstone.

Interpretation.—This facies association consists of tide-influenced deposits of a lagoonal setting. This is based on the limited lateral extent,

the bidirectional paleocurrent indicators, and the vertical transition from flaser, through wavy, to lenticular bedding. The sheltered lagoonal setting is inferred from the absence of wave indicators (Fan et al. 2013). The trace-fossil assemblages are consistent with the interpretation of a restricted bay or lagoonal setting with variable salinity (MacEachern and Bann 2008). The distal exposures (location 6; Fig. 2) record a sandier setting closer to the lagoon margin.

FA7: Marine-Influenced Distributary Channels

Description.—FA7 consists of fine-grained cross-stratified sandstone beds (10–30 cm thick) with undulatory bed boundaries (facies 14), parallel lamination (facies 10), sporadic thinly interbedded siltstone ripples (facies 12), and rare double mud drapes. Individual sandstone bodies have overall thickness of 1.5–2 m and are bounded by erosional, lower concave-upward surfaces. Paleocurrent data reveal a scattered pattern covering 360° variance (Table 2). Based on these data, it was not possible to reconstruct the true width from individual sandstone bodies, but an approximation is in the order of 30 m. Bioturbation is low (BI 0–2, *Skolithos*), non-uniformly distributed, but predominant in the lower parts

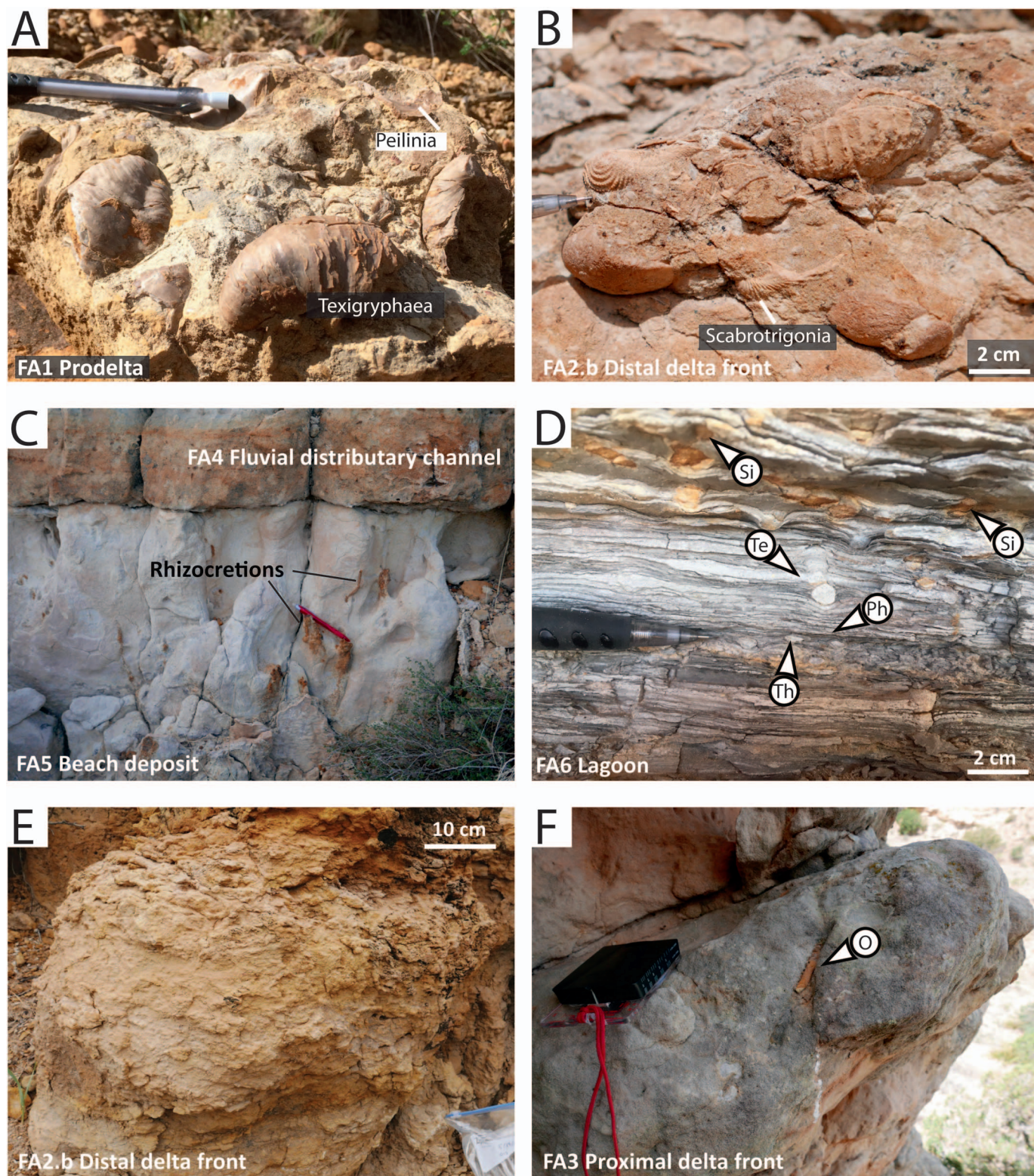


Fig. 5.—Photographs of selected macrofauna and ichnology with their associated facies associations (Table 2). **A**) Lower-shoreface macrofauna *Texigryphaea* and *Peilinia levicostata* oyster genera in (> 20 cm) sandy prodelta stormbeds (FA1). **B**) Middle-shoreface faunal association (*Scabrotrigonia*–*Turritella*) in distal to proximal delta-front sandstone (FA2, FA3). **C**) Rhizcretions and poorly developed pedogenesis at the top of a 3-m-thick beach deposit (FA5). **D**) Lenticular bedding with sporadic bioturbation (BI 1–4), in lagoonal deposits (FA6). **E**) Cleaning- and coarsening-upward, highly bioturbated (BI 5–6), distal delta-front sandstone (FA2.b). **F**) Non-bioturbated to poorly bioturbated (BI 0–1), fine- to medium-grained proximal delta-front sandstone (FA3). Te, *Teichichnus*; Th, *Thalassinoides*; Ph, *Phycosiphon*; Si, *Siphonichnus*; O, *Ophiomorpha*. 15-cm pencil and 8-cm compass for scale.

TABLE 2.—Summary of main facies associations and their constituting lithofacies in the study area. Schematic log represents main depositional environments. Vertical stacking is a simplified 2D representation of 3D stratigraphic arrangement. Note: thickness is not to scale but is adjusted to fit text. BI, bioturbation index (Taylor and Goldring 1993). For locations, see Figure 2. All rose diagrams have a north-up orientation. Note that FA2 and FA3 have a combined rose diagram.

Facies Association		Description	Distribution & dimensions	Interpretation
FA8	<p>Interdistributary bay n = 11</p>	Predominantly brownish-gray muddy siltstone (facies 17) with a few structureless sandstone beds (facies 5), locally rippled bed tops. Coarsening-upward and thickening to cross-stratified and erosionally based fine-grained sandstone (facies 9).	Present throughout study area. Eroded by FA4 and FA7. The < 1.5-m-thick coarsening-upward packages extend laterally up to few tens of meters. Facies 5 beds (5–15 cm thick) extend 100–200 m along strike.	Bayhead deltas, splay deposits, and interdistributary fines in a subaqueous lower-delta-plain setting.
FA7	<p>Marine-influenced distributary channel n = 28</p>	Upward-fining sand-bodies with cross-stratification, parallel lamination, occasional trough cross-stratification, undulatory bed boundaries (facies 8, 9, 10, 14). Moderate marine influence (mud-drapes, <i>Skolithos</i> ichnofacies, BI 0–3).	Multilateral, multistory (2–3) channel bodies, found within muddy siltstones of FA8. Composite thickness < 3 m. Width < 50 m.	Marine-influenced distributary channels with varying tidal modulation (Channel type IV). Deposition within upstream limits of sea-level influence.
FA6	<p>Lagoon</p>	Interbedded sandstones and siltstones (facies 2, 3, 4). BI 0–3 in sandstone beds (<i>Skolithos</i> ichnofacies) and BI 3–4 in the lenticular interval (<i>Cruziana-Skolithos</i> ichnofacies). Bidirectional ripples.	Present only in southern part of study area (location 5, 6), average thickness of 5 m. The section in location 6 is more sand-prone and the only place where roots are observed. FA6 is incised by FA4.	Vertical transition from flaser, through wavy, to lenticular bedding. Deposition in a sheltered, tide-influenced environment.
FA5	<p>Beach n = 5</p>	White to light-gray parallel-laminated and low-angle or tangential cross-stratified sandstone (facies 9, 10) dipping both paleolandward and seaward. Locally weak pedogenesis and/or bioturbated by roots or <i>Skolithos</i> (BI 0–3).	Tabular, 1.5–3 m thick, up to 2 km along depositional dip. Progressively fragmented and eventually absent. Erosionally overlain by FA4.	Deposition of foreshore and backshore sands with occasional wash-over fans, rooted eolian dunes and short-lived marine incursions.
FA4	<p>Fluvial distributary channel n = 145</p>	Erosionally based, channelized fining-upward, with an infill of cross-stratified sandstone, occasional trough cross-stratified (facies 8, 9). Parallel- and ripple-laminated sandstones (facies 10, 12) in the upper part. Locally, basal lag of conglomerate and wood debris (facies 16). Rarely, disorganized sandstone and back-flow ripples (facies 11, 16) at the channel base.	Channel type I) Continuous distributary-channel sheet, < 4 m thick Channel type II) Multilateral channel bodies, embedded within interdistributary fines (FA8) Channel type III) Multistory composites, 8–12 m thick, 90–250 m wide.	Channel type I) Laterally amalgamated fluvial distributary channels Channel type II) Isolated fluvial distributary channels Channel type III) Incised valley
FA3	<p>Proximal delta front n = 26</p>	Gradual continuation of FA2, cross-stratified, trough cross-stratified, and parallel lamination (facies 8, 9, 10) with non-uniform BI 0–3 (<i>Skolithos</i> ichnofacies). Current and wave ripple-laminated sandstone (facies 12, 13) only locally. Coal flakes in uppermost beds.	Sheet forming throughout study area, consisting of amalgamated lensoid geometries. Incised by FA4 in most places.	Coalesced fluvial-dominated mouth bars. The low and non-uniform BI-trend results from relatively stressed living-conditions because of river proximity.
FA2	<p>Distal delta front</p>	FA 2.a) Cross-stratified, current and wave ripple-laminated sandstone (facies 9, 13). Local mud-draped unidirectional ripples (facies 4). FA 2.b) Upwards decreasing BI values (<i>Cruziana</i> ichnofacies; BI 4–6 to 2) (facies 7). Repetitive 5–15-cm-thick normally graded sandstone beds (facies 5) mainly in the lower part. Local shell beds (facies 6).	FA2.a) Sheet forming. Interfingers with FA 2.b. Occurs at locality 2 and 6. FA2.b) Sheet forming throughout study area (except locality 6). Tabular, 10–50-cm-thick shellbeds only at locality 1 and 2. FA 2.a and 2.b grade vertically into FA3.	Deposition above fair-weather wave-base. FA2.a) distal delta front - stressed depositional conditions FA2.b) distal delta front - unstressed depositional conditions. Cleaning- and coarsening-upward sand. Episodic high-discharge events.
FA1	<p>Prodelta</p>	Fossiliferous dark gray fissile mudstone (facies 1) with several thin (10–20 cm) sandstone beds (facies 6, 7) present in the upper half of the fine-grained interval. Base consists locally of a pebble lag (facies 16).	Vertically and laterally gradational into distal delta-front facies (FA2). FA1 is 9–20 m thick, present throughout the study area. Tabular, 50–100-cm-thick bioturbated sandstone beds (facies 7) are at least 2 km along dip.	Deposition in a prodeltaic setting, below fair-weather wave-base. Local preservation of a transgressive lag. The bioturbated sand- and shell-beds represent short-lived storm deposits.

of sandstone bodies. Syneresis cracks and *Teredolites*-bored wood fragments are rare, but oxidized roots are common. FA7 is embedded stratigraphically within FA8.

Interpretation.—This facies association represents marine-influenced distributary channel-deposits with minor tidal modulation. This is based on the bioturbation, syneresis cracks, *Teredolites*-bored wood fragments, and locally preserved tidal indicators (i.e., double mud drapes). Deposition occurred close to the shoreline where mixing of fresh and saline waters occurred at times of decreased river discharge. These brackish-water conditions allowed only limited bioturbation and low-diversity ichnofauna (MacEachern et al. 2005).

FA8: Interdistributary-Bay Deposits

Description.—Gray-brown muddy siltstone of FA8 occurs throughout the study area and exhibits only purple mottling in the most proximal part (location 1; Fig. 2). Very fine- to fine-grained, thin (0.1–0.4 m), tabular sandstone beds are traceable for 100–200 m along depositional strike and locally show *Skolithos* trace fossils (BI 0–2). These sandstone beds are commonly structureless but can locally exhibit cross-stratification, and they are interbedded with rippled siltstone (Fig. 5B). Additionally, minor thin coarsening-upward successions (< 50 cm thick) grade from silty mudstone into interbedded very fine-grained sandstone with gray, thin silty mudstone layers. These are in turn overlain by erosionally based cross-stratified or structureless sandstone bodies (facies 5, 9). Isolated sandstone

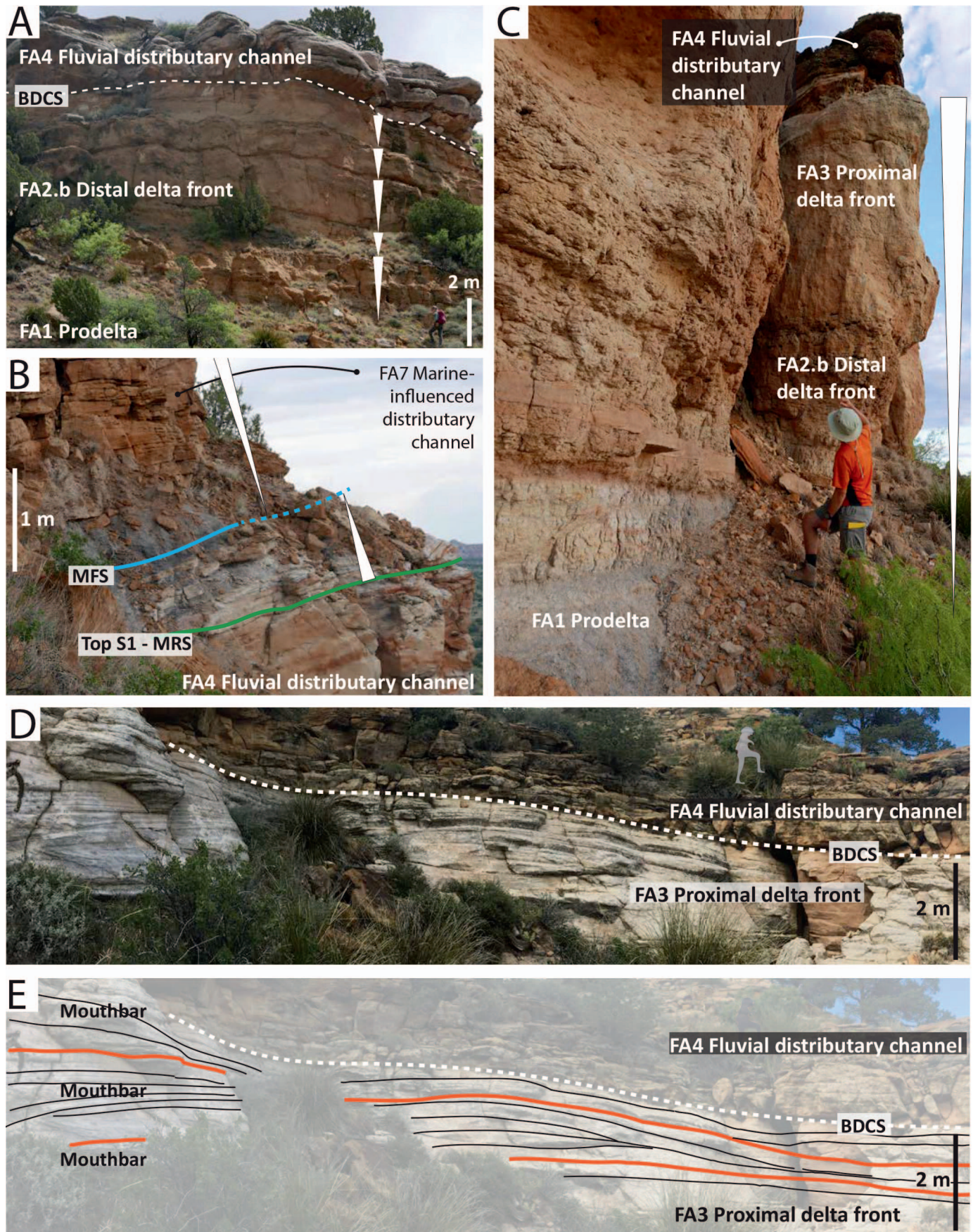


FIG. 6.—Photographs of vertical facies successions and selected architectural elements. **A**) Stacked coarsening-upward sequences in an unstressed delta-front environment facies association (FA2.b), overlain by fluvial distributive channel deposits (FA4). **B**) Example of key stratigraphic surfaces separating coarsening- and fining-upward

bodies of FA4 (fluvial distributary channel) and FA7 (marine-influenced distributary channel) occur in FA8.

Interpretation.—FA7 represents interdistributary-bay deposits. The muddy siltstone does not coexist with any coal deposits, and signs of weak pedogenesis are documented only in the most proximal part of the study area (location 1; Fig. 2). The thin-bedded sheet sandstone deposits are interpreted as crevasse-splay or overbank-flow deposits. The limited thickness of the coarsening-upward packages, their limited lateral extent, and the presence of overlying fluvial facies suggest localized shallowing-upward events. These strata may represent bayhead deltas and distal bay infill (e.g., Aschoff et al. 2018).

VERTICAL FACIES SUCCESSIONS

The vertical and lateral relationships between facies associations reveal key stratigraphic surfaces, which help define three genetically related packages in the studied succession (Figs. 7, 8): one coarsening-upward deltaic succession (S1) and two coarsening-upward successions consisting of lower-delta-plain and beach deposits (S2, S3). These successions reflect successive regressive depositional pulses, but they are not preserved everywhere due to erosion following late Neogene uplift (Dolliver 1985).

Two distinct geographical zones are identified based on marked differential thicknesses (Fig. 8). Zone 1 (locations 1, 2, 3) contains a ~15-m-thick coarsening-upward succession, S1. Zone 2 (locations 5, 6) is characterized by an ~7-m-thick coarsening-upward succession, S1, overlain by lagoonal deposits. Location 4 is situated in the transitional area between the zones.

Succession S1: From Prodelta to Delta Plain

Facies associations FA1–4 (Table 2) form a typical coarsening-upward and shallowing-upward deltaic succession. The basal ravinement surface is part of the Tucumcari Shale lower boundary (e.g., Lucas and Kisucky 1988). The thickness of the overlying sandstone-rich package (FA2–4) varies throughout the study area with a maximum of 20 m in the northern part and a minimum of 7.5 m in the southern part. Here, lagoonal deposits (FA6) conformably overlie distributary-channel-belt (FA4) strata. The coarsening-upward package (FA2, FA3) represents delta-front deposits and an upward filling of paleo-water depth and/or increase in sand supply. This package forms a laterally extensive sheet-like sandstone, interpreted to result from successive coalescence of mouth bars. The high-index bioturbation challenges the identification of onlapping and/or converging mouth-bar or lobe strata in most cases, because of its obliterating effect. Lensoid geometries are more easily identifiable in nonbioturbated strata (Fig. 6D). Truncation surfaces show a stepwise configuration in the transitional area between Zones 1 and 2 and represent minor down-steps of the delta front (Fig. 8C). FA4 represents a sand-filled distributary-channel belt (Fig. 8B–C) and locally the top is significantly rooted. Continuous lateral amalgamation of distributary channels is typical for the S1 succession, and it also comprises (10–12 m thick) multistory channel bodies which incised deeply into the underlying deltaic deposits (Fig. 8C).

Successions S2 and S3: Coastal and Lower-Delta-Plain Successions

The overlying successions (S2, S3, each 4–5 m thick) represent overall shallowing-upward packages. They comprise a laterally varying spectrum

of facies including fluvial and marine-influenced distributary channels (FA4, FA7), beach (FA5), and interdistributary-bay deposits (FA8). Both S2 and S3 successions are dominated by muddy siltstone (FA8). A thin (0–40 cm) layer of brackish-marine mudstone is commonly present at the base of S2 and S3, the top of which is interpreted as a maximum flooding surface (Fig. 6B). The top of S2 and S3 is formed of crevasse-splay deposits, small bayhead deltas, or channel bodies. The latter display either fully fluvial (FA4) or marine-influenced (FA7) elements and are arranged in laterally disconnected channel belts. In the S2 succession, a few multistory channel bodies (8–10 m thick) incise deeply into underlying strata. In S3, muddy siltstone (facies 17, FA8) is dominant. No beach or lagoonal deposits (FA5, FA6) are present, and bayhead deltaic strata, crevasse splays (FA8), and channel belts (FA4) are less significant than in S2.

Both S2 and S3 represent a very dynamic coastal setting in which sedimentary patterns relate to the laterally varying influence of river and marine processes. Deposition in a mostly subaqueous setting is interpreted based on the marine-influenced sandstone bodies and near absence of roots. The abundant fluvial strata and rare occurrence of rooted surfaces suggest a significant fluvial component and occasional subaerial conditions.

KEY STRATIGRAPHIC SURFACES

Maximum Regressive and Flooding Surfaces

Description.—Fluvial strata form the top of all the shallowing-upward successions in the study area (Fig. 8). Continuous lateral amalgamation of sand-filled-channel belts is typical for succession S1, whereas they become progressively more isolated up section (through S2 and S3). In the proximal part of the study area (location 2; Fig. 2), the top surface of succession, S1 (MRS1, Figs. 7, 8), shows evidence of local oxidation. In the central part of the study area (location 3; Fig. 2), deposits overlying the MRS1 consist of ~50 cm of finer-grained sandstone interbedded with mudstone, which in turn is overlain by ~50 cm of dark gray mudstone (MFS, Figs. 6B, 7, 8C). In Zone 2 (Fig. 8C), 4-m-thick lagoonal deposits (FA6) overlie this top surface. The top surfaces of successions S2 and S3 (MRS2 and MRS3) mark the top of shallowing-upward packages as well. MRS2 is intensely rooted in Zone 1 and records subaerial conditions.

Interpretation.—All surfaces bounding the shallowing-upward successions are overlain by more distal facies and are commonly represented by a sandstone–mudstone contact. Roots and oxidation suggest subaerial exposure. These surfaces correspond to the end of a regressive phase and are therefore interpreted as maximum regressive surfaces (MRS1, MRS2, MRS3; Fig. 7). Maximum regressive surfaces represent a change from progradational to retrogradational stacking patterns, irrespective of controlling parameters. Such surfaces also mark a turnaround in the balance between sediment supply and accommodation, and hence the turning point from shoreline regression to transgression (e.g., Helland-Hansen and Martinsen 1996; Embry 2002; Catuneanu 2006). The lack of marine influence in the upper fluvial strata of succession S1 suggests deposition during late highstand or falling stage rather than (late) lowstand aggradation (Holbrook and Bhattacharya 2012). In the central part of the study area (location 3; Fig. 2), transgressive marine facies (i.e., indicative of deepening) separate the underlying MRS from the maximum flooding

packages. A layer of brackish-marine mudstone represents a regional flooding event. **C**) Coarsening-upward deltaic succession consisting of prodelta (FA1), distal (FA2.b), and proximal (FA3) delta-front deposits overlain by fluvial distributary channels (FA4). Note the lack of clear bed boundaries, the sand dominance, and the difference from the clear coarsening-upward sequences of Part A. **D**) Outcrop picture of fluvial distributary channels (FA4) in erosional contact with proximal delta-front sands (FA3). **E**) Interpretation of Part D, with stacked mouth bars based on the presence of lensoid-bar geometries. MFS, maximum flooding surface; MRS, maximum regressive surface; BDCS, basal distributary composite scour; S1, coarsening-upward succession 1. Triangles indicate grain-size trends.

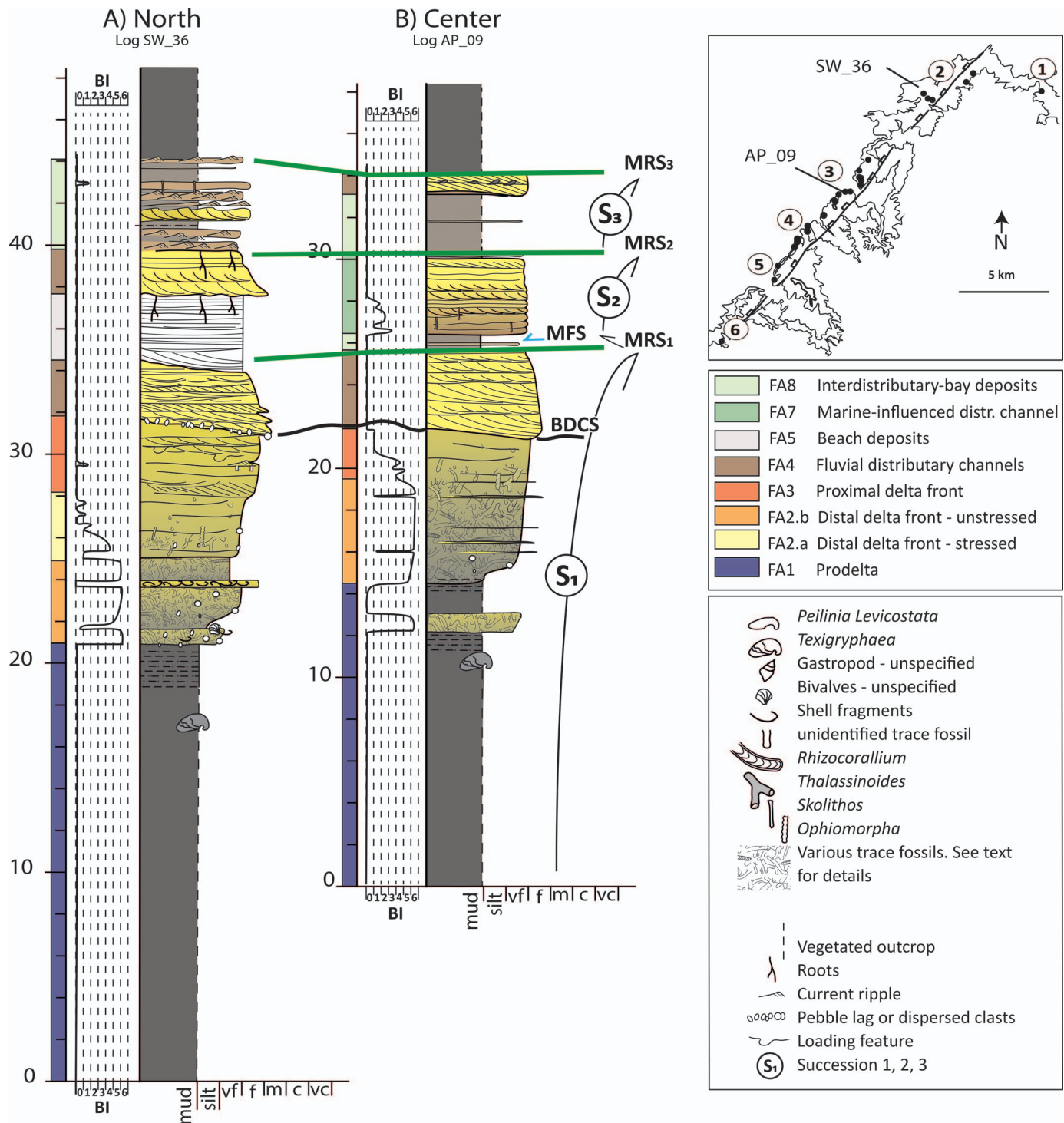


FIG. 7.—Stratigraphic logs illustrate typical vertical facies successions and the most significant differences between the **A**) northern (location 2) and **B**) central (location 3) parts of the study area (Fig. 2). Delta-front sediments in Log A and Log B represent stressed (FA2.a) and unstressed (FA2.b) delta-front depositional conditions, respectively. Key stratigraphic surfaces that can be traced across the study area are shown between the logs. Where transgressive deposits are not preserved, the MRS coincides with the MFS. Map shows study area outline with locations of depicted logs. MRS, maximum regressive surface; MFS, maximum flooding surface; BDCS, basal distributary composite scour; BI, bioturbation index. Defined coarsening-upward successions (S₁, S₂, S₃) are further described in the text.

surface (MFS) (Fig. 6B). Where transgressive deposits are not preserved, the MRS coincides with the MFS.

Downstepping delta-front strata at location 4 (Fig. 8C) and the thinner S₁ succession at locations 5 and 6 (Fig. 8C) place MRS₁ lower in Zone 2

compared to Zone 1 (Fig. 8C). In locations 3–6, lagoonal deposits overlie the MRS₁ and indicate a local inundation due to along-strike depositional variability. This contrasts with the sharp and distinctive character of MRS₂ and MRS₃. The discontinuous nature of MRS₃

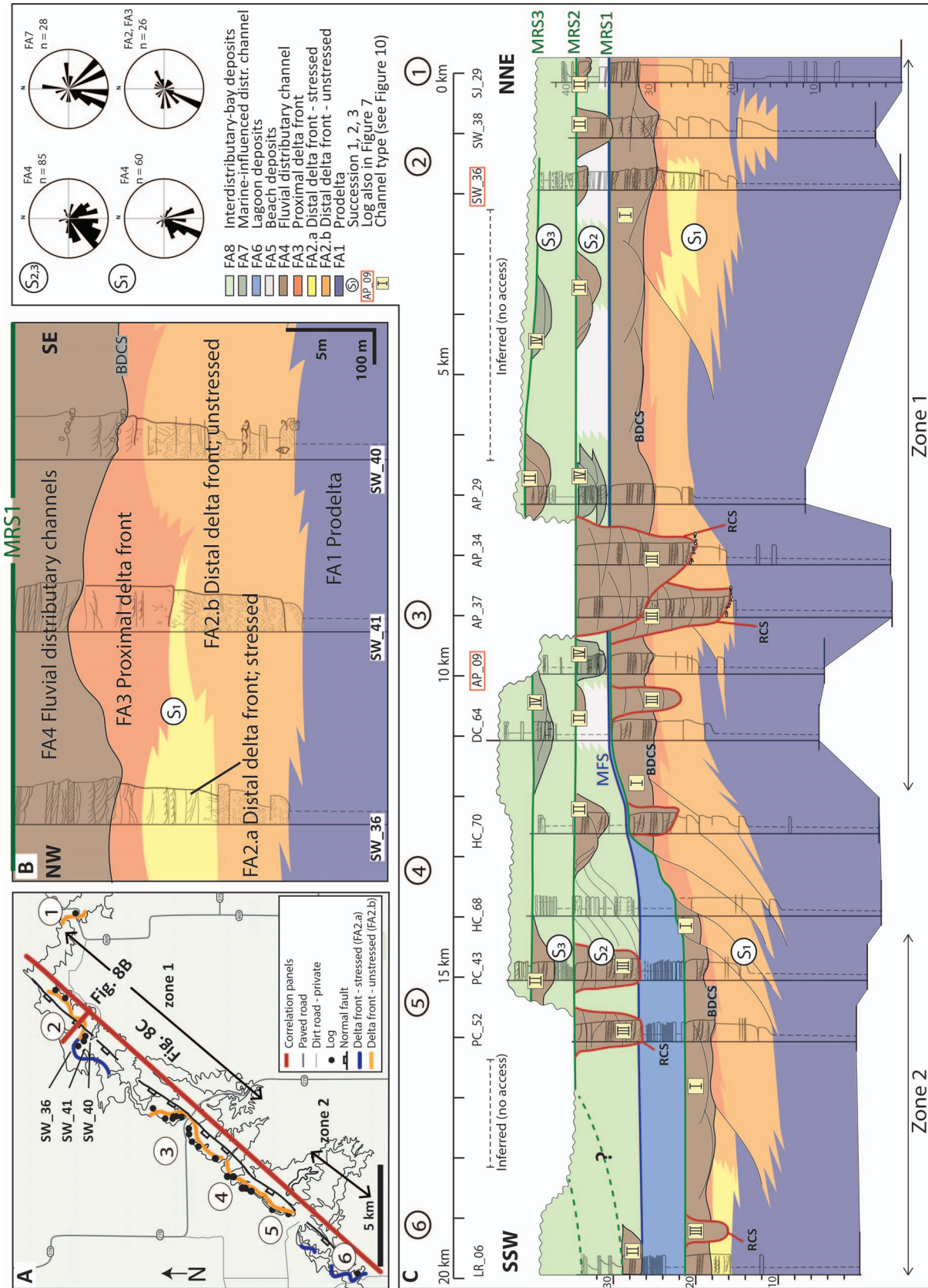


FIG. 8.—**A**) Map of study area with distribution of stressed (FA2.a) and unstressed (FA2.b) delta-front depositional conditions. **B**) Strike-oriented correlation panel of succession S1 showing intraparasquence variation of stressed delta-front environments (FA2.a) vs unstressed delta-front environments (FA2.b). **C**) Correlation panel from NNE (paleolandward) to SSW (paleoseaward) with ~ 1 km spacing between available log data with interpreted facies associations and key stratigraphic surfaces. Note the thickness changes between Zone 1 and Zone 2 and the rare absence of fluvial distributary-channel deposits (FA4) in the S1 succession. The Tucumcari Shale base cannot be used as a datum. The stratigraphic levels with continuous (S1) and laterally discontinuous (S2) distributary-channel deposits (FA4) are used as a datum. A higher proportion of fine-grained and hence more compacted sediments in the lagoonal deposits (FA6) could explain the lower position of the MFS in Zone 2. Southward-inclined clinoform geometries are observed in location 3, but are otherwise inferred from delta-front thickness changes or downstepping. MRS, maximum regressive surface; MFS, maximum flooding surface; RCS, regional composite scour; BDCS, basal distributary composite scour.

suggests possible interfingering with the paralic strata of the overlying Pajarito Formation, in addition to differential erosion related to late Neogene uplift (Dolliver 1985).

Large-scale Erosional Composite Surfaces

Two types of erosional composite surfaces are distinguished in the study area; those bounding i) sheets of amalgamated distributary-channel deposits (FA4) (Fig. 6, 8C), and ii) multistory infill of incised valleys (FA4) (Fig. 8C).

Interpretation.—The basal surfaces of amalgamated distributary channel deposits mark sharp facies boundaries that represent the typical shallowing-upward character of deltaic successions. They form a composite scour that results from persistent deposition and avulsion of distributaries that over time covered the delta plain with distributary-channel fills. These distributaries are younger than the deltaic deposits into which they incise and feed a more distal part of the delta system. They are however contemporary with the regressive succession recording the discrete down-stepped shoreline wedges of which they are part (Fig. 8C). In this study, their basal composite surface is termed a *basal distributary composite scour* (BDCS). These surfaces are similar to the type 3.D “shoreface-incised channels” described by Pattison (2018). BDCSs differ from surfaces at the base of shoreface-incised channels in that they form more laterally extensive scours and are infilled with fluvial distributary deposits (FA4) that lack marine indicators. Like the surfaces of Pattison (2018), however, they are localized to discrete shoreface deposits. They are not part of the regional scour surface cut by trailing trunk channels that forms the regional sequence-bounding scour.

In contrast, the erosional composite surfaces bounding the multistory infill of incised valleys separate fully fluvial facies from underlying distal to proximal deltaic facies associations, and are a local component of the regional sequence-bounding scour. They represent a basinward shift in depositional facies caused by advance of fluvial trunk channels over older regressive delta phases. This abrupt facies dislocation implies a surface of sequence stratigraphic importance and meets many criteria for a sequence boundary, as defined by Van Wagoner et al. (1988) and Zaitlin et al. (1994). Based on observations, however, the surface is diachronous along strike. This relates to formation by the action of laterally shifting erosion and deposition by a river (e.g., Blum and Price 1998; Holbrook 2001; Strong and Paola 2008). In down-dip direction, the basal surface of the river extends seawards and is diachronous as well (e.g., Strong and Paola 2008; Bhattacharya 2011). In this study, the erosional composite surfaces bounding multistory incised-valley infill are termed *regional composite scours* (RCSs) (Holbrook and Bhattacharya 2012). These surfaces are also incised into the underlying coastal wedge but extend beyond the scale of a single down-stepped wedge in the falling-stage to lowstand systems tracts. They differ from the BDCSs, which are confined to discrete down-step events. These regional composite surfaces correlate to sequence-bounding scours cut by trailing channels farther up dip in northeastern New Mexico and Colorado (Holbrook 1996; Holbrook et al. 2006).

CLINOFORMS

Description.—At location 2, distal and proximal delta-front deposits (FA2.b, FA3) of the S1 succession exhibit clinoforms at location 2 (Fig. 2, 9). The outcrop orientation (N–S) is slightly oblique to the mean paleocurrent direction throughout the study area (SSW, Fig. 2). Clinoforms here consist of coarsening-upward, very fine- to fine-grained sandstone with a vertical decrease in bioturbation index and bed boundaries that become more distinct towards the top. Fluvial processes eroded the paleoshoreline break, thereby eliminating the possibility for trajectory analyses (Helland-Hansen and Gjelberg 1994). Clinoform foresets reveal

steeper dip angles (~ 6 to 8°) in the upper part, and downlap onto lower-angle (~ 2 to 4°) clinoform foresets (Fig. 9). The former have lengths of ~ 25 m whereas the latter can be traced from the proximal delta front to their shale-out point over a distance of ~ 180 m.

Clinothems in the S2 succession (Fig. 8C) reveal several 1–2-m-thick heterolithic sandstone bodies that occur within interdistributary fines (facies 8). Clinoforms here have lengths of approximately 25–50 m and dip (~ 6 to 10°) in the same direction as the S1 clinoforms. The internal architecture reveals onlapping and downlapping relationships, and mound-shaped geometries with a lateral extent of approximately 10 m in places.

Interpretation.—Clinothems in succession S1 represent two sets of mouth bars (Fig. 9). Upwards-increasing dip angles in mouth-bar beds are related to deposition just before mouth-bar abandonment (Enge et al. 2010) or increased proximity to the river mouth (e.g., Fidinini and Ghinassi 2016). The measured dip of 2° resembles common clinoform dips for sandy shoreline deltas (e.g., Olariu et al. 2010; Patruno et al. 2015), although several studies of river-dominated delta deposits have documented steeper dips, such as the Aberdeen Member (3 – 7°) and Ferron “Notom” delta (6 – 7°) (Charvin et al. 2010 and Li et al. 2011, respectively).

Clinothems in the study area were deposited in an estimated water depth of 15–20 m. This estimate takes into account the erosion of the shoreline break, accommodation for the thickest documented clinothems, and an additional 0–5 m uncertainty resulting from the general position of rollover points below sea level in sandy shoreline deltas (Patruno et al. 2015). Clinoform geometries in the S1 succession are observed only at location 2 (Fig. 2, 9), and their occurrence coincides with a rapid thickening of the succession. The rareness, steepness, and the abrupt thickening are interpreted to reflect a localized deepening in the underlying basin topography. We suggest that the common Mesa Rica delta front clinoforms are kilometer-scale, low-angle clinoforms that are difficult to resolve from outcrop-data (e.g., Anell et al. 2016), and that the smaller-scale clinoforms that could be documented are an exception (Fig. 9). Determination of lobe size is also hampered by the consistent sandy nature and lack of onlapping and/or converging strata at visible scales and conditions.

Clinothems in succession S2 reveal multiple, vertically stacked, thinner mouth-bar sets. Their heterolithic nature suggests a higher A:S ratio (e.g., Ainsworth et al. 2017) than succession S1 clinothems, but other factors such as differential grain size, relative densities of incoming and ambient fluids, and process regimes cannot be discarded (e.g., Postma 1990; Orton and Reading 1993; Bhattacharya 2006). Detailed investigation of these is beyond the scope of this paper.

FLUVIAL ARCHITECTURE

Four different types of channel deposits (FA4, FA7) are distinguished based on sandstone-body dimensions and vertical and lateral spatial arrangements (Fig. 10). Focus is on the architectural significance, and overlapping FA descriptions are avoided.

Channel Type I: Fluvial Distributary-Channel Sheet

Description.—Channel type I consists of laterally amalgamated distributary-channel fills (FA4) that form a nearly continuous sheet in the S1 succession throughout the study area (Figs. 8C, 10). Most channel fills are single story and in lateral erosional contact with each other forming multilateral bodies (*sensu* Potter 1967). Two-story fills are locally present in Zone 1 (Fig. 8C). Lateral-accretion elements are mostly absent. Paleocurrent measurements reveal a SSW dominance with a spread of ca.

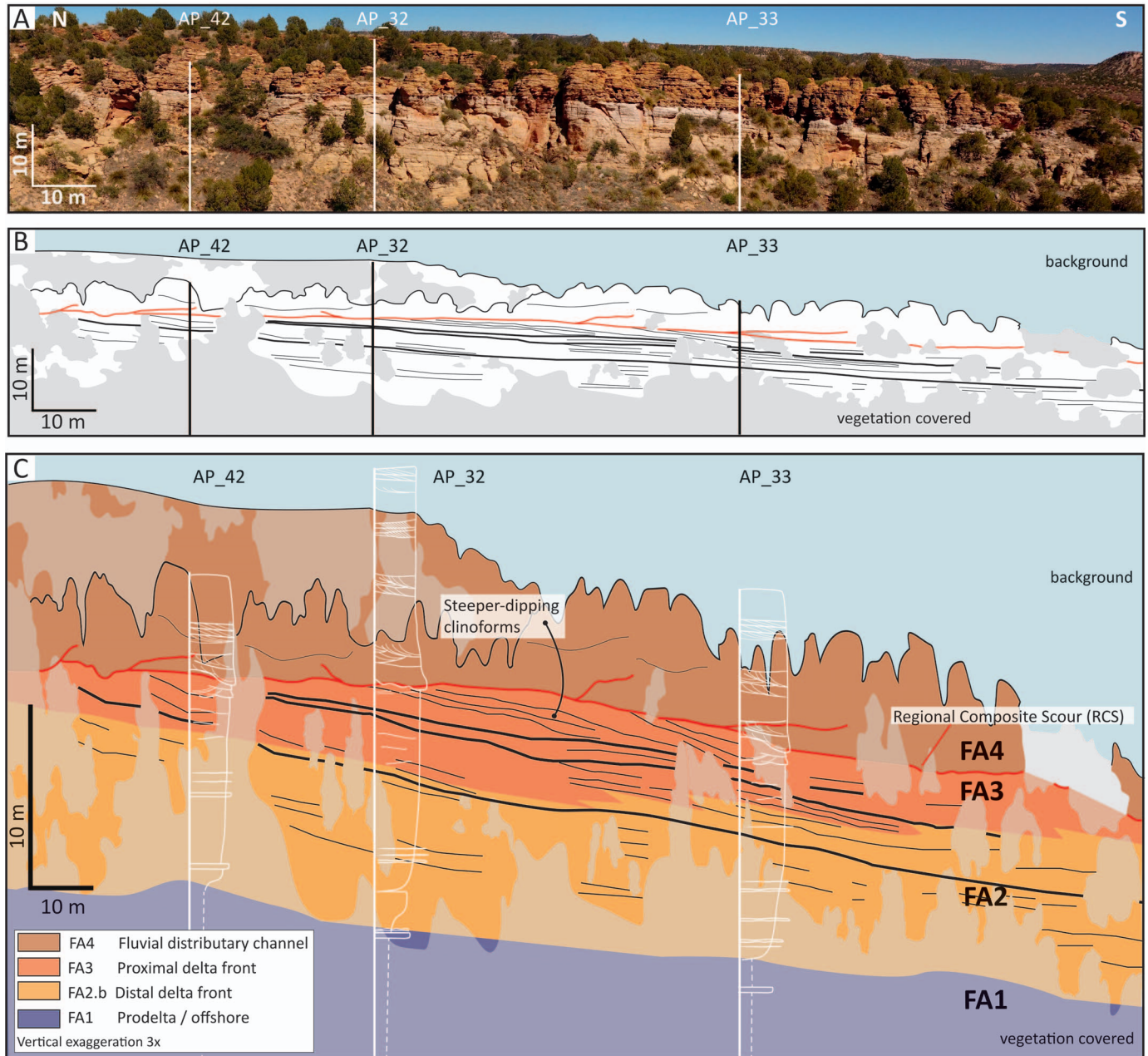


FIG. 9.—**A**) Photopanel of clinoforms recognized in Apache Canyon (see location 3 in Fig. 2). **B**) Line drawing of Part A with logging locations indicated. Traceable clinoform surfaces are marked. **C**) FA interpretation from sedimentary logs overlaid onto vertically exaggerated (3 \times) pane. Distal delta-front sediments (FA2) grade upwards into proximal delta-front (FA3) sediments. The contact with the overlying fluvial sandstone (FA4) is erosional and forms a regional composite scour (RCS). The clinoform foresets reveal steeper dip angles (~ 6 to 8°) in the upper part, and downlap onto the underlying lower-angle (~ 2 to 4°) clinoform foresets.

90° (Fig. 8C). Their basal bounding surfaces form a basal distributary composite scour (BDCS).

Interpretation.—Channel type I represents sand-filled amalgamated distributary channels on a delta plain. Its sheet-forming character, the absence of any marine indicators, and the lack of interfluvial deposits suggest an upper-delta-plain environment and overall low-accommodation setting. The absence of accretionary elements is interpreted as deposition by low-sinuosity channels with lateral deposition by avulsion rather than lateral migration (cf. Holbrook 1996).

Channel Type II: Isolated Fluvial Distributary Channel

Description.—Channel type II consists of individual channel-fill elements (FA4, 1–4 m thick) form amalgamated multilateral channel bodies embedded within interdistributary fines (FA8) (Figs. 8C, 10). Most bodies are single-story, but there are composite bodies comprising up to three stories that are separated by erosional surfaces. The channel-fill elements are present both as independent channels and as channel fills adjacent to point-bar elements. The combination of the latter, their isolated character within the interdistributary fines, and the generally single-story

stacking pattern sets them apart from other channel-fill deposits in this study.

Interpretation.—Channel type II represent distributary-channel-belt deposits in an upper-delta-plain setting. The presence of lateral-accretion surfaces indicates channel sinuosity (e.g., Miall 1985). Their local multistory character is interpreted as reoccupation of a preferred channel path and potentially represents lower-order distributaries. The multilateral nature suggests that there was limited accommodation on the delta plain (e.g., Miall 2014) and that a preferred stream location existed for longer periods of time between major distributary channel-belt avulsions. However, the isolated nature and sinuous channel pattern suggest a higher A:S ratio (i.e., more accommodation or less sediment supply) or a more proximal location along the depositional profile than during deposition of the fluvial distributary sheet (channel type I).

Channel Type III: Incised Valley

Description.—Isolated and thicker (8–12 m), multistory channel bodies (FA4) exist at two stratigraphic levels throughout the study area, and incise deeply into underlying strata (Figs. 8, 10, 11). These multistory bodies are bound by an erosional composite surface and have total widths between 90 and 250 m. Individual channel-fill elements average 4–5 m in thickness (max. 9 m thick) in the axial part and become thinner towards the margins, forming multilateral bodies. Dune-scale trough and tabular cross-stratification is up to 1.30 m thick in the axial part, whereas bed thicknesses are < 50 cm at the margins. The multistory channel bodies contain smaller elements in their upper parts characterized by root marks and a lack of evidence of marine influence. In places, the multistory infill consists of stacked compound bars with similar thicknesses (Fig. 11). Here, the uppermost two stories display a dominance of channel-fill elements that exist both independently and adjacent to bar forms.

Interpretation.—The erosional composite surfaces at the bases of multistory infills represent a regional composite surface. The successive stacking of compound bars (Fig. 11) indicates a predominantly aggradational infill and repeated occupation of the same topographic low. Erosion and deposition occurred at depths greater than one bankfull channel depth below the topographic surface (e.g., Strong and Paola 2008; Martin et al. 2011). The cut-and-fill character of the topmost stories suggests successive avulsion and abandonment of smaller distributaries. This consistent multistory and multilateral channel-body nature strongly suggests that they represent incised valleys (Holbrook 2001; Fielding 2008). The absence of multiple internal sequence boundaries or terrace structures classifies them as simple valleys (Zaitlin et al. 1994; Holbrook 2001). In experimental modeling studies, autogenic formation of valleys was limited to the proximal reaches of a deltaic system (Muto and Steel 2004) and up-dip of the delta apex (Strong and Paola 2008). This supports the interpretation that a drop in base level played a role in the formation of the incised valleys recorded in this study.

Channel Type IV: Marine-Influenced Distributary Channel

Description.—This channel type occurs in fine-grained interdistributary strata (FA8) and comprises marine-influenced channel bodies (FA7) (Figs. 8C, 10). These consist of amalgamated multilateral stacked channel sheets that average 3–4 m thick, in which individual channel-fill elements have an average thickness of 1.5–2 m (Fig. 10). These sandstone bodies typically contain two or three stories. Marine indicators progressively diminish towards the top of the channel infill, where oxidized roots are locally present.

Interpretation.—Channel type IV represents marine-influenced distributary channels that record progressively diminishing marine influence towards the top and therefore a shallowing and/or progradational trend. This is based on the upper part of the channel fills commonly lacking marine indicators, and the roots indicating (nearly) emergent conditions. The isolated occurrence of multistory channel bodies within interdistributary fines (FA8) is similar to channel type II and suggests similar depositional conditions. However, channel type IV bodies were deposited within the landward limits of marine influence (Paola and Mohrig 1996), whereas channel type II bodies were deposited upstream of marine influence.

DISCUSSION

Dominant Process Regime at the Delta Front

In succession S1, an important difference exists between subtle lensoidal internal geometries (Fig. 6D, E), typical of poorly bioturbated distal delta-front deposits (FA2.a), and extensive tabular geometries, typical for highly bioturbated delta-front sandstone bodies (FA2.b). The latter is the dominant delta-front expression throughout the study area. Both expressions form extensive sandstone sheets despite their different internal geometries. The delta-front deposits have characteristics that are typical for both river and wave processes acting on the delta front, whereas tidal indicators are scarce. The continuity of distributary-channel deposits (FA4) is a critical indicator for a strong river influence. Proximal delta-front deposits (FA3) may form mound-shaped geometries and are devoid of wave-induced bedforms, which is also common for deposition in front of river-outlets with a strong fluvial influence (e.g., Bhattacharya 2006; Gani and Bhattacharya 2007).

Wave influence is inferred from high bioturbation indices in distal delta-front sandstone deposits (FA2.b), given that wave agitation optimizes infauna living conditions (MacEachern et al. 2005; MacEachern and Bann 2008; Gani et al. 2009). Wave influence is also consistent with the common configuration into tabular geometries of these deposits, which results from lateral sand redistribution. However, it is unlikely that waves acted as a primary depositional sediment-sourcing mechanism because the delta-front deposits (FA2.a and FA3) do not resemble beach or strandplain deposits. The sheet-like Mesa Rica delta-front deposits are therefore interpreted as the product of initial deposition dominated by river influence, followed shortly after by minor wave reworking. The wave-reworked sediment is derived from the associated fluvial feeder systems and not from sediment introduced by longshore transport. In a river-dominated deltaic setting, wave influence can nevertheless dominate freshwater river inflow at times of decreased discharge or abandonment, and thereby create a substrate-colonization window (MacEachern et al. 2005; MacEachern and Bann 2008; Gani et al. 2009), which allows high bioturbation indices. It is ambiguous as to whether minor wave reworking occurred during inactive phases of mouth-bar deposition or after the abandonment of complete mouth bars or lobes (i.e., complexes of mouth bars).

Coalesced Mouth Bars and Highly Avulsive Distributary Channels

The striking sandy nature of the coalesced Mesa Rica mouth-bar deposits contradicts the general concept of river-dominated deltaic sandstone deposits being interbedded with mudstone resulting from deposition during periods of low discharge (e.g., Posamentier and Morris 2000; Bhattacharya and Giosan 2003). In addition, delta-front sheet geometries are classically assigned to wave-dominated deltas (e.g., Wright and Coleman 1973; Bhattacharya and Giosan 2003). Here we propose a depositional model (Fig. 12) for the Mesa Rica delta in which a high-frequency avulsion pattern of distributary channels results in sheet-forming coalesced mouth bars and lobes without the dominance of wave redistribution processes.


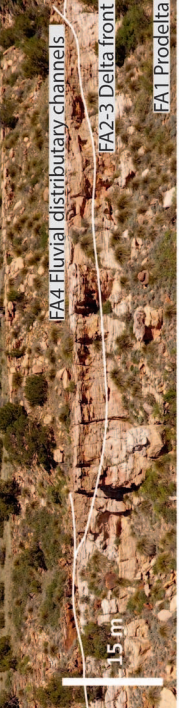



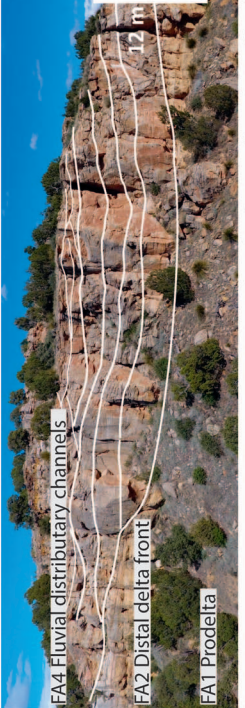
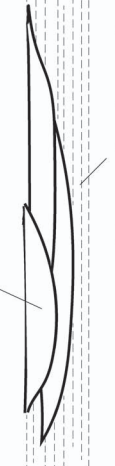

	W : T (m)	Stacking pattern	Main characteristics & Sketch	Field example
<p>Type I - Fluvial distributary channel sheet</p>	<p>Average: 70 : 4 Max: 150 : 6</p>	<p>Mostly 1 story Multi-lateral</p>	<p>FA4 Fluvial distributary channels</p>  <p>- No lateral-accretion elements - Forms continuous sheet</p>	 <p>Stan's Windturbines (location 2, Fig.2)</p>
<p>Type II - Isolated fluvial distributary channels</p>	<p>Average: 50 : 2,5 Max: 150 : 7</p>	<p>Mostly 1 story Max 3 stories Multi-lateral</p>	<p>FA4 Fluvial distributary channels</p>  <p>FA8 Interdistributary fines</p> <p>- Independent channels and adjacent to lateral-accretion elements - Isolated within interdistributary fines</p>	 <p>Apache Canyon (location 3, Fig.2)</p>
<p>Type III - Incised valley</p>	<p>Average: 140 : 10 Max: 250 : 12</p>	<p>Multi-story Multi-lateral</p>	<p>FA4 Fluvial distributary channels</p>  <p>- Scarce lateral-accretion elements - Isolated, scoured into deltaic sediments</p>	 <p>Apache Canyon (location 3, Fig.2)</p>
<p>Type IV - Marine-influenced distributary channels</p>	<p>Average: 30 : 2 Max: 50 : 3</p>	<p>2 - 3 stories Multi-lateral</p>	<p>FA7 Marine-influenced distributary channels</p>  <p>FA8 Interdistributary fines</p> <p>- No lateral-accretion elements - Isolated within interdistributary fines - Tide / marine influenced</p>	 <p>Apache Canyon (location 3, Fig.2)</p>

Fig. 10.—Summary of interpreted channel types, their dimensions, and characteristics. The sketch generalizes the field observations and is not solely based on the displayed field example. The incised-valley field example (Type III) is interpreted in higher resolution in Figure 11. W:T (width:thickness) ratios are given for individual channel elements, except for channel type III, where it refers to the total composite dimensions.

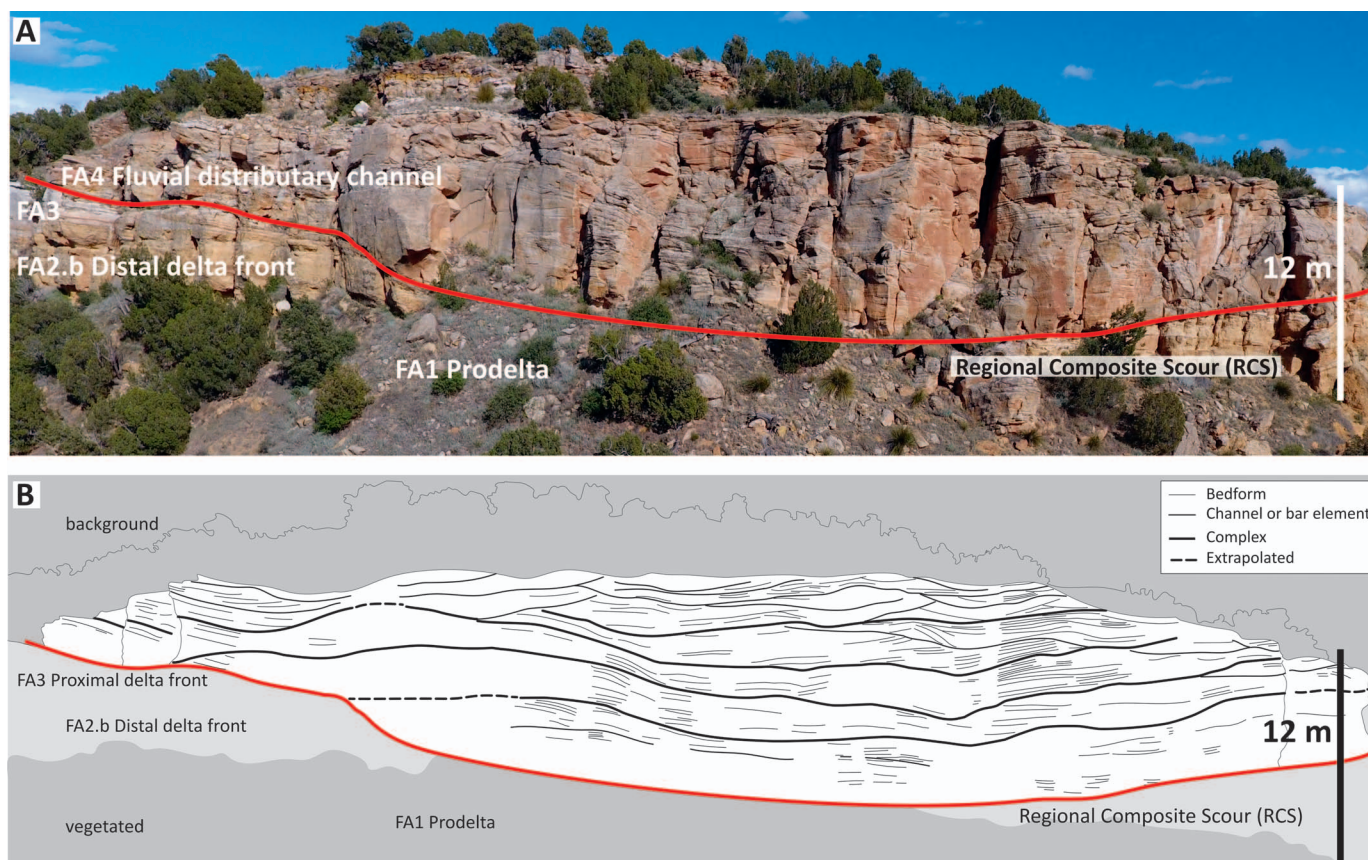


Fig. 11.—**A**) Photopanel and **B**) line drawing of a multistory channel body. The erosional regional composite scour (RCS) bounds a multistory infill composed of stacked bar forms and channel elements (FA4). The uppermost stories consist of mainly cut-and-fill channel elements with locally adjacent barforms. Underlying distal deltaic deposits (FA2.b) are sparsely exposed. Prodelta mudstones (FA1) are mostly covered by vegetation. The main paleocurrent direction is into the outcrop.

What caused the highly avulsive character of the Mesa Rica mouth bars? We believe that the low accommodation combined with high supply of sandy sediment are crucial for this process. With high discharge, bedload accumulation at a river mouth can exceed the redistribution capacity of longshore transport and cause local loss of wave energy by damping the wave impact. This leads to increased sediment concentration in the river mouth, which eventually increases deposition in the channel and leads to bifurcation (e.g., Holbrook 1996; Edmonds and Slingerland 2007; Davidson et al. 2013; Anthony 2015).

Low-accommodation conditions additionally favor lengthening of the longitudinal profile during delta progradation, thereby lowering the gradient and inducing straightening of distributary channels (references in Holbrook 1996). Channel filling occurs when sediment load exceeds the carrying capacity because of increased frictional processes. Experimental studies by Bryant et al. (1995) suggest that increased sedimentation rates induce increasing avulsion frequencies. Edmonds and Slingerland (2007) demonstrate with numerical modeling that mouth-bar progradation stops when the water depth over the river mouth bar is equal to or less than 40% of the inlet depth. The river flow is diverted around the bar, and a new bifurcation is formed. The low-accommodation setting accelerates the mechanisms that trigger bifurcation and avulsion because less sediment is needed to reach the critical bar thickness for bifurcation.

In the Mesa Rica, the numerous coexisting river outlets formed mouth bars that went through successive depositional cycles (i.e., deposition, extension, avulsion, and abandonment, *sensu* Olariu and Bhattacharya (2006)), with short recurrence intervals. Typical inter-avulsion times reported from modern deltas vary significantly (e.g., Jerolmack and

Mohrig (2007)). The Mesa Rica high-frequency avulsion pattern is inferred based on the observed sheet geometries, but its rate cannot be quantified. During mouth-bar depositional cycles, fluvial, tidal, and wave processes are competing forces controlling sediment deposition and distribution. River jets can have a damping effect on waves and tides at times of high discharge (Anthony 2015). However, interaction of river jets with waves can also suppress mouth-bar formation (Jerolmack and Swenson 2007) which causes only a few channels to develop in the distributary network. This situation does not match the abundant distributary channels observed in the Mesa Rica delta and thus supports the argument that wave reworking of the delta-front sediment was only minor.

A minor role of wave reworking suggests also that most sand was deposited in front of the river outlet. Together with high sediment supply, these conditions led to channels becoming clogged with sand, hence promoting bifurcation and eventually avulsion if channels close completely (Slingerland and Smith 2004). The record of nearly continuous deposits of amalgamated distributary channels on the Mesa Rica delta top suggests that avulsion was probably more common than bifurcation. The low depositional gradient and high sediment supply forced repeated mouth-bar depositional cycles and feeder-channel deposition, which eventually resulted in occupation of every part of the delta plain by distributary channels and the formation of a basal distributary composite scour (Fig. 8C, 12). Long-lasting progradation facilitated this persistent pattern.

Modern analogues for the Mesa Rica delta have their limits, since Holocene deltas have experienced constant sea-level rise on a millennial timescale since their initiation about 8000 years ago, and have since had a comparatively short time to create sheet-forming distributary channel

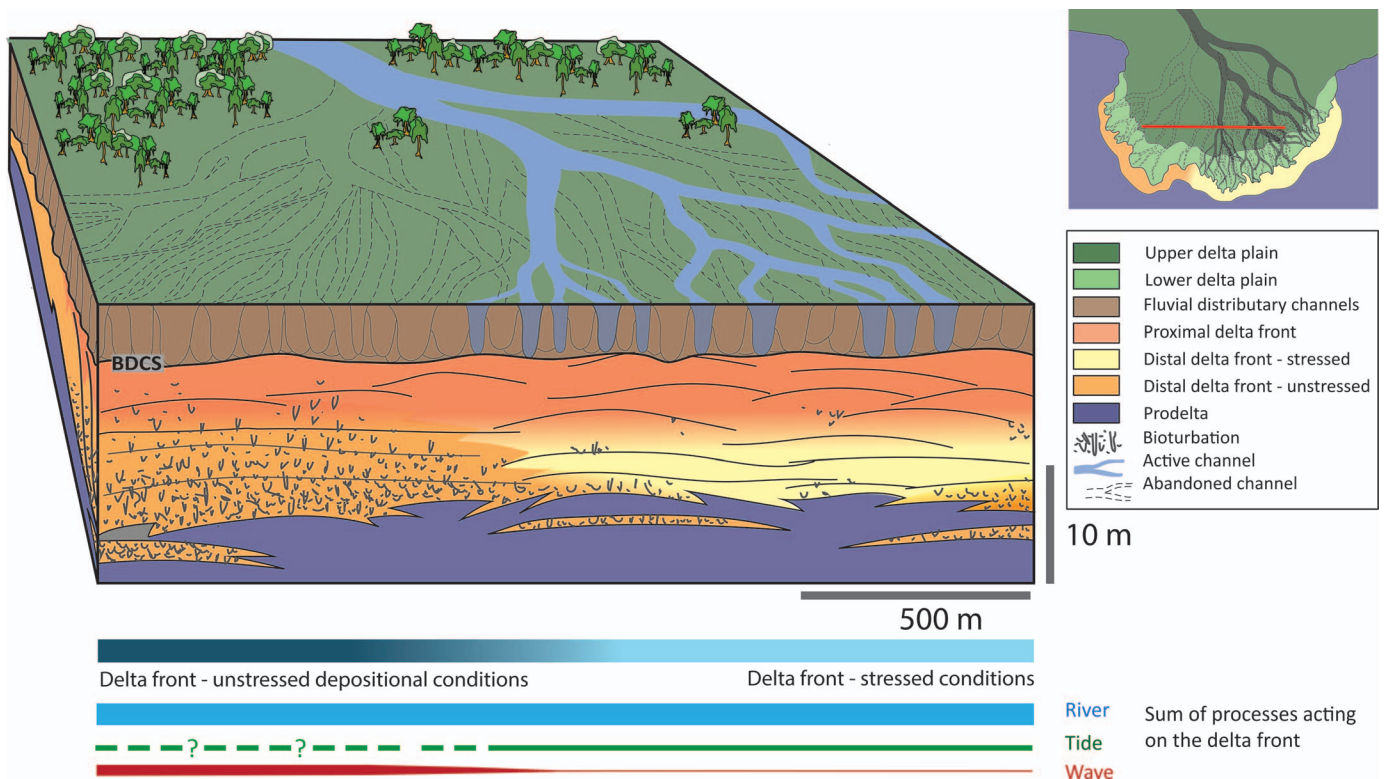


FIG. 12.—Conceptual model for coalesced delta-front sheet sandstone development from highly avulsive distributary channels. Laterally amalgamated sand-filled distributary channels overlie delta-front deposits which are characterized by their consistent sandy nature. The straightened low-gradient channels cause frictional processes to increase, hence inducing channel-fill deposition and subsequent bifurcation and/or avulsion. Additionally, the low accommodation acts as an amplifier for the interrelated processes of highly avulsive distributaries and recurring mouth-bar development cycles at short time scales. Shortly after deposition, minor wave reworking facilitated lateral sand redistribution and favored faunal living conditions resulting in highly bioturbated sandstone beds. The sum of processes active on the delta front varies in strike orientation as a result of the competition between fluvial, tidal, and wave processes during deposition. See text for further discussion. BDCS, basal distributary composite scour.

deposits. The Volga delta is characterized by a low gradient (5×10^{-5}) with delta distributaries bifurcating rapidly (Overeem et al. 2003). This has led to significant erosion and deposition of sand-filled distributaries on the delta plain. This process is expected to continue with prolonged progradation and has the potential to further cover the delta plain with amalgamated distributary-channel deposits.

An End-Member Example of Low-Accommodation Deltaic Deposition

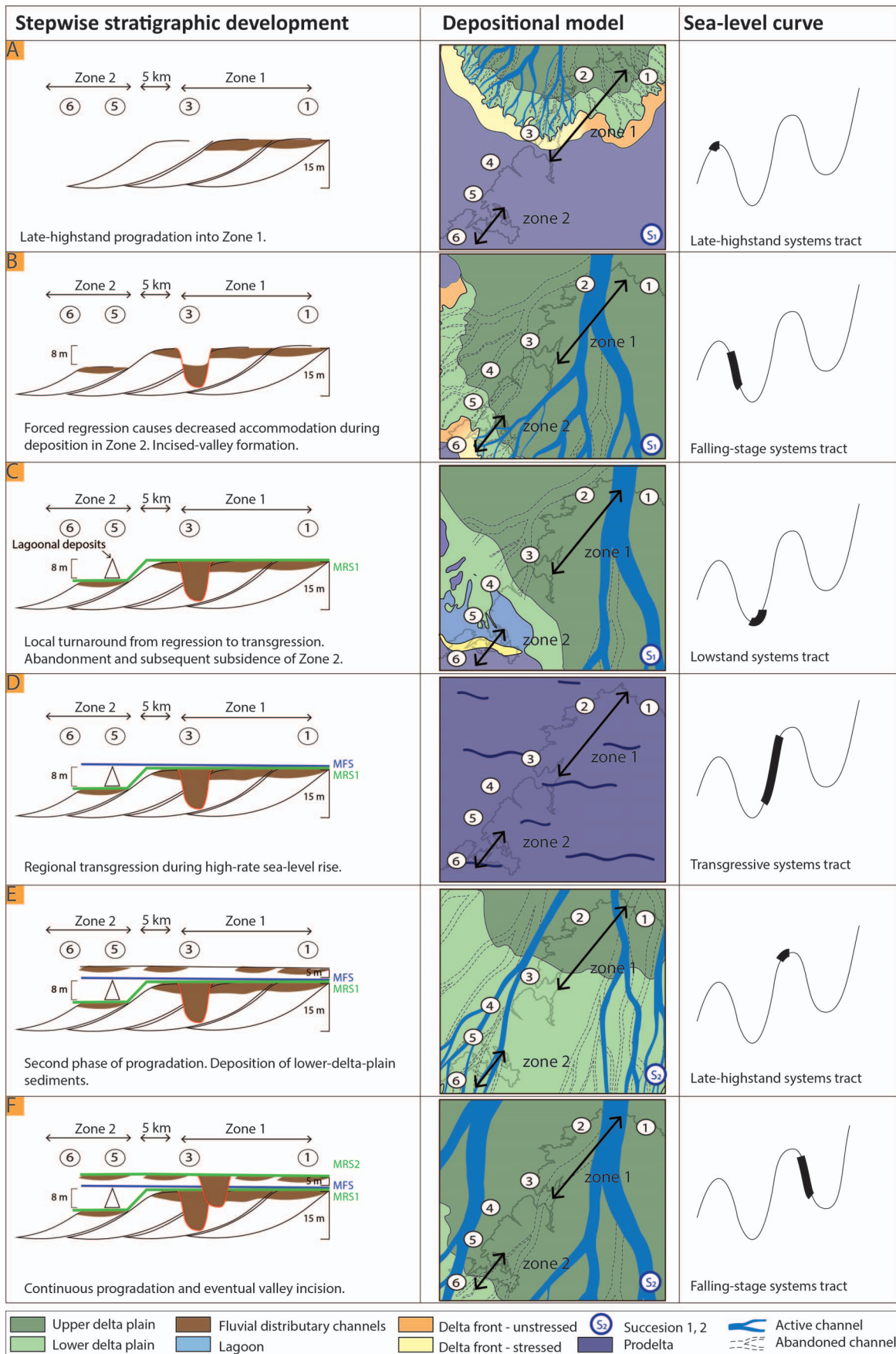
Existing models for deltaic deposition in low-accommodation settings highlight the lateral-stacking mechanisms (e.g., Ainsworth et al. 2017) with a resultant lobate delta morphology (Olariu and Bhattacharya 2006). When combined with high sediment discharge, this results in laterally extensive sand bodies because of the decreasing distance between channels and the merging of proximal mouth-bar deposits. We propose that the S1 succession of the Mesa Rica delta is an end-member example of this concept, when considering ratios of accommodation to sediment supply (A:S). End members of low-accommodation deltas are either very mud-prone or very sand-prone. Commonly used examples of ancient low-accommodation deltas are the Panther Tongue (e.g., Olariu et al. 2005), several depocenters of the Ferron Sandstone (e.g., Bhattacharya and Tye 2004; Garrison and Van den Bergh 2004), the Perrin Delta (e.g., Brown et al. 1990; Olariu and Bhattacharya 2006), and the Horseshoe Canyon Formation (e.g., Ainsworth et al. 2017). The first is significantly more heterolithic than the Mesa Rica delta, and therefore represents a higher A:S ratio. The intermittent and isolated nature of distributary channels in both the Ferron Sandstone and the Horseshoe Canyon Formation is also

different from the record of continuous amalgamation of these in the Mesa Rica delta. Because of the predominant sandy nature of the Mesa Rica delta-front deposits and the fluvial occupation of nearly every part of the delta plain, the Mesa Rica delta is interpreted as a sand-rich end member within the low-accommodation spectrum.

Paleogeographic Reconstruction and Forcing Mechanisms

The following are the key aspects of our paleogeographic reconstruction of the deltaic Mesa Rica. First, a lobate-delta model is inferred from the nearly sheet-forming deposits of amalgamated distributary channels at the delta top (succession S1) and deposition in a low-accommodation setting. Second, two discrete geographical zones (Zone 1 and Zone 2; Fig. 8, 13) are distinguished based on differential succession thicknesses: Zone 1 contains the ~ 15 -m-thick coarsening-upward S1 succession, whereas Zone 2 is characterized by an ~ 7 -m-thick coarsening-upward S1 succession that is overlain by lagoonal deposits (transitional area is located in between Zones 1 and 2). Third, multistory channel bodies are interpreted as incised-valley fills.

Progressive progradation of a large-scale lobate delta with multiple outlets and distributary channels into Zone 1 (Fig. 13A) was accompanied by a high frequency of mouth-bar formation, abandonment, and reactivation. The highly amalgamated character and lack of marine influence in the fluvial distributary channels that formed the delta-top (succession S1) suggests that these were deposited during late highstand or earliest falling stage (Fig. 13A, B). Continued progradation during forced regression led to downstepping delta-front deposits and progres-



sively less accommodation during deposition in the transitional area and Zone 2 (Fig. 13B). Forced regression caused highstand delta-front exposure, a steepened river slope, and initiation of valley formation near the contemporary shoreline (Talling 1998; Holbrook et al. 2006). A combination of abandonment of Zone 2 and early sea-level rise (Fig. 13C) created localized transgressive conditions favoring the development and preservation of a lagoonal setting (e.g., Bhattacharya 2010). This implies that the location of active deltaic progradation switched spatially and deposition continued contemporaneously. Continued progradation beyond the outcrop limits of this study during earliest sea-level rise is highly likely, although not proven here. Deposition of the deltaic coarsening-upward succession S1 consumed most of the accommodation that was present in the Tucumcari Basin at the time of deposition, and was followed by a transgression that is recorded throughout the study area (Fig. 13D). A second progradational phase (succession S2) took place and sediment routing into the study area was reactivated. Deposition occurred in a dynamic lower-delta-plain setting in which short-lived marine incursions locally allowed weak tidal influence and the preservation of bayhead deltas. Weak pedogenesis is recorded in Zone 1, which supports our upper-delta-plain interpretation (Fig. 13E). Continued progradation during successive forced regression caused incision into the coastal prism and thus valley formation (Fig. 13F). The main paleocurrent trend of SSW mimics the NE–SW-elongated basin center (Fig. 14), and supports an important link between basin configuration and regional depositional trend (Kisucky 1987; Holbrook and Dunbar 1992; Holbrook and White 1998).

Autogenic forcing, as another possible control, is considered for the stratigraphic development described above as well. However, autogenic formation of the observed incised valleys with stacked multistory bar forms is unlikely (Strong and Paola 2008). These valleys are close to the terminal shoreline, and backwater effects would promote deposition and avulsion rather than incision (Blum et al. 2013). The downstepping delta front and thin S1 succession in Zone 2 cannot be explained by early abandonment and subsequent compaction because it is the youngest part of the outcropping delta deposits. Additionally, documented changes in relative sea level (Oboh-Ikuenobe et al. 2008) support the sequence-stratigraphic framework as established in the upstream part of the system (e.g., Holbrook 1996; Holbrook 2001). Based on the identified stratigraphic surfaces, incised valleys, flooding surfaces, and presence of three depositional cycles, successions S1 and S2 correlate to the respective lower and upper Mesa Rica Sandstone, as defined and described in Scott et al. (2004) and Oboh-Ikuenobe et al. (2008). The S3 is likely the distal equivalent of the overlying Pajarito Formation and Romeroville Sandstone. Consequently, these sequence stratigraphic surfaces extend up dip over distances of more than ~ 300 km and cannot be explained by autogenic behavior in the Tucumcari Basin.

Finally, ascribing all the observations to either solely autogenic or allogenic forcing is unreasonable, because a combination of controls at different time and spatial scales is most plausible (Hampson 2016). Low-accommodation settings enhance autogenic dynamics and make it more difficult to decipher the difference between system-induced sedimentary processes and changes in allogenic conditions.

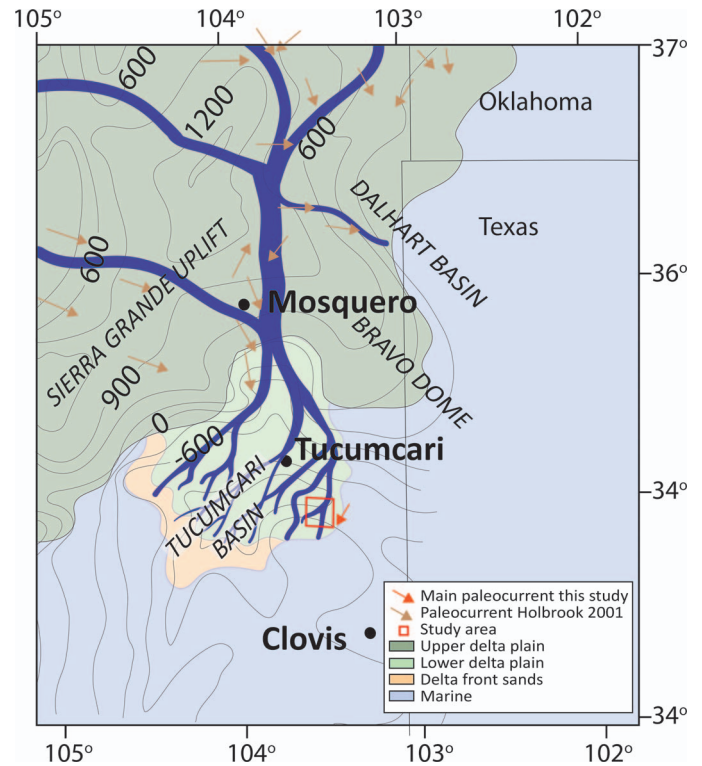


FIG. 14.—Influence of basin topography on depositional trends. Interpretation of paleoshoreline based on Holbrook and Dunbar (1992), Holbrook and White (1998), and Precambrian basement outline (Suleiman and Keller 1985). Location of the Tucumcari Shale pinchout is used to interpret the most upstream deltaic reaches. Deflection of the main paleocurrent trends (brown arrows) in the Tucumcari Basin is inferred from the orientation of the basin center (NE–SW) and the average paleocurrent trends from this study (orange arrow), which mimics the basin orientation. Structural contour map of Precambrian basement (contour interval is 300 feet; ~ 92 m) is modified from Suleiman and Keller (1985). Brown paleocurrents are from Holbrook (2001).

CONCLUSIONS

- For the first time, a detailed facies and architectural analysis has been published for the shallow-marine part of the Cenomanian Mesa Rica Sandstone, a low-accommodation, thin and sandy deltaic system that drained into the Western Interior Seaway. The studied interval preserves three phases of progradation into the Tucumcari Basin. The oldest phase (succession S1) comprises a sheet-forming deltaic coarsening-upward succession deposited in maximum 20 m water depth. Subsequent phases (successions S2 and S3) took place under progressively less accommodation.
- The Mesa Rica delta is interpreted as the product of initial deposition dominated by river influence, followed shortly after by minor wave reworking. This is based on the extensive units of closely spaced

FIG. 13.—Sequential paleogeographic reconstruction of the Mesa Rica shoreline in the study area. The left, middle, and right columns represent a simplified version of the correlation panel throughout the study area (Fig. 8C), the interpreted depositional model, and relative sea-level curve, respectively. **A**) Progressive progradation of a lobate delta with numerous outlets and distributary channels into Zone 1. The lobate model is based on Olariu and Bhattacharya (2006). Distributaries are younger than the deltaic deposits into which they incise and feed a more distal part of the delta system. **B**) Continued progradation during forced regression causes decreased accommodation during deposition in Zone 2 and formation of incised valleys. **C**) Earliest sea-level rise combined with abandonment of Zone 2 creates localized transgression, resulting in preservation of a lagoonal setting. **D**) Flooding of the study area during relative sea-level rise. **E**, **F**) Second phase of progradation and reactivation of sediment routing throughout the study area, resulting in deposition of sediments assigned to the coarsening-upward succession S2 with eventual incised-valley formation. See text for further discussion.

distributary-channel deposits, and high degrees of bioturbation and configuration into tabular geometries of deltaic sandstones.

- A depositional model for the Mesa Rica delta is proposed, in which a high-frequency avulsion pattern of distributary channels is the major driving mechanism behind the development of coalesced mouth bars and lobes. Both high sandy-sediment supply and low accommodation had key roles in accelerating mouth-bar evolution by hampering the redistribution potential of waves and promoting bifurcation and avulsion. The low accommodation acted as an amplifier for the interrelated processes of frequent avulsion of distributaries and recurring mouth-bar development cycles at short time scales. It also favors straightening of distributary channels and increased frictional processes at the river bed, hence causing rapid infill of newly formed channels.
- Highly avulsive distributary channels produced a mappable and extensive basal surface referred to here as the basal distributary composite scour (BDCS). This surface resembles a sharp, within-trend, facies-bounding surface that separates distributive fluvial strata and underlying proximal deltaic strata along a laterally extensive scour. This surface is confined to discrete down-stepped shoreline wedges, and is thus not a regional sequence-bounding scour. The surface contrasts with the regional composite scours (RCSs) that underlie incised valleys, record shoreface incision during forced regression, extend beyond single down-stepped wedges, and are part of the regional sequence boundary.
- Mesa Rica deltaic sandstone body geometries are similar to those described for classic wave-dominated environments. This can be particularly relevant for subsurface studies, because it cautions against interpretations of amalgamated wave-dominated shoreline systems based solely on sandstone geometries, without taking into account the possible limited preservation potential and postdepositional modification of primary deltaic characteristics. This study provides a sand-rich end-member example of deltaic deposition in a low-accommodation setting, when considering accommodation to sediment supply (A:S) ratios.

ACKNOWLEDGMENTS

Funding was allocated to the field expeditions by the Lower Cretaceous Arctic (LoCra consortium). Sincere thanks goes to Stephen Hasiotis for essential feedback on ichnology determination, and Wolfram Kürschner for assistance with processing and analyzing palynology samples. We thank Lina Hedvig Line, Cody Myers, Blake Warwick, and Edwin Tieman for field assistance, and Gretchen Gurtler and Axel Hungerbuehler from the Mesalands Dinosaur Museum and Natural Sciences Laboratory in Tucumcari for irreplaceable logistic help. We thank Karl Charvin, Cornel Olariu, Paul Myrow, and Gary Hampson for their thorough reviews and editorial comments. Last, but definitely not least, we thank the many ranchers who permitted us access to their private lands, with a special thanks to Tom Mackechnie.

REFERENCES

ABOUELRESH, M., AND SLATT, R., 2011, Shale depositional processes: example from the Paleozoic Barnett Shale, Fort Worth Basin, Texas, USA: *Open Geoscience*, v. 3, p. 398–409.

AINSWORTH, R.B., VAKARELOV, B.K., AND NANSON, R.A., 2011, Dynamic spatial and temporal prediction of changes in depositional processes on clastic shorelines: toward improved subsurface uncertainty reduction and management: *American Association of Petroleum Geologists, Bulletin*, v. 95, p. 267–297.

AINSWORTH, R.B., VAKARELOV, B.K., MACÉACHERN, J.A., RARITY, F., LANE, T.I., AND NANSON, R.A., 2017, Anatomy of a shoreline regression: implications for the high-resolution stratigraphic architecture of deltas: *Journal of Sedimentary Research*, v. 87, p. 425–459. doi:10.2110/jsr.2017.26

ALLEN, J.P., AND FIELDING, C.R., 2007, Sequence architecture within a low-accommodation setting: an example from the Permian of the Galilee and Bowen basins, Queensland, Australia: *American Association of Petroleum Geologists, Bulletin*, v. 91, p. 1503–1539.

ANELL, I., LECOMTE, I., BRAATHEN, A., AND BUCKLEY, S.J., 2016, Synthetic seismic illumination of small-scale growth faults, paralic deposits and low-angle clinoforms: a case study of the Triassic successions on Edgeøya, NW Barents Shelf: *Marine and Petroleum Geology*, v. 77, p. 625–39.

ANTHONY, E.J., 2015, Wave influence in the construction, shaping and destruction of river deltas: a review: *Marine Geology*, v. 361, p. 53–78.

ANTIA, J., AND FIELDING, C.R., 2011, Sequence stratigraphy of a condensed low-accommodation succession: Lower Upper Cretaceous Dakota Sandstone, Henry Mountains, southeastern Utah: *American Association of Petroleum Geologists, Bulletin*, v. 95, p. 413–447.

ASCHOFF, J.L., OLARIU, C., AND STEEL, R.J., 2018, Recognition and significance of bayhead delta deposits in the rock record: a comparison of modern and ancient systems: *Sedimentology*, v. 65, p. 62–95.

BHATTACHARYA, J.P., 2006, Deltas, in Posamentier, H.W., and Walker, R.G., eds., *Facies Models Revisited*: SEPM, Special Publication 48, p. 237–292.

BHATTACHARYA, J.P., 2010, Deltas, in James, N.P., and Dalrymple, R.W., eds., *Facies Models 4*: Geological Association of Canada, p. 233–264.

BHATTACHARYA, J.P., 2011, Practical problems in the application of the sequence stratigraphic method and key surfaces: integrating observations from ancient fluvial–deltaic wedges with Quaternary and modeling studies: *Sedimentology*, v. 58, p. 120–169.

BHATTACHARYA, J.P., AND GIOSAN, L., 2003, Wave-influenced deltas: geomorphological implications for facies reconstruction: *Sedimentology*, v. 50, p. 187–210.

BHATTACHARYA, J.P., AND TYE, R.S., 2004, Searching for modern Ferron analogs and application to subsurface interpretation, in Chidsey, T.C., Jr., Adams, R.D., and Morrison, T.H., eds., *Analog for Fluvial–Deltaic Reservoir Modeling: Ferron Sandstone of Utah*: American Association of Petroleum Geologists, *Studies in Geology*, v. 50, p. 39–58.

BHATTACHARYA, J.P., AND WALKER, R.G., 1991, Allostratigraphic subdivision of the Upper Cretaceous Dunvegan, Shaftesbury, and Kaskapau formations in the northwestern Alberta subsurface: *Bulletin of Canadian Petroleum Geology*, v. 39, p. 165–191.

BHATTACHARYA, J.P., AND WILLIS, B.J., 2001, Lowstand deltas in the Frontier Formation, Powder River basin, Wyoming: implications for sequence stratigraphic models: *American Association of Petroleum Geologists, Bulletin*, v. 85, p. 261–294.

BUKERK, J.F., EGGENHUISEN, J.T., KANE, I.A., MEIJER, N., WATERS, C.N., WIGNALL, P.B., AND MCCAFFREY, W.D., 2016, Fluvio-marine sediment partitioning as a function of basin water depth: *Journal of Sedimentary Research*, v. 86, p. 217–235. doi:10.2110/jsr.2016.9

BLAKEY, R.C., 2014, Paleogeography and paleotectonics of the Western Interior Seaway, Jurassic–Cretaceous of North America: *American Association of Petroleum Geologists, Search and Discovery Article*, no. 30392.

BLUM, M.D., AND PRICE, D.M., 1998, Quaternary alluvial plain construction in response to glacio-eustatic and climatic controls, Texas Gulf coastal plain, in Shanley, K.W., and McCabe, P.J., eds., *Relative Role of Eustasy, Climate, and Tectonism in Continental Rocks*: SEPM, Special Publication 59, p. 31–48.

BLUM, M., MARTIN, J., MILLIKEN, K., AND GARVIN, M., 2013, Paleovalley systems: insights from Quaternary analogs and experiments: *Earth-Science Reviews*, v. 116, p. 128–169.

BROADHEAD, R.F., 2004, Petroleum geology of the Tucumcari Basin: overview and recent exploratory activity: *New Mexico Geology*, v. 26, p. 90–94.

BROWN, L.F., SOLIS-IRIARTE, J.R., AND JOHNS, D.A., 1990, Regional depositional systems tracts, paleogeography, and sequence stratigraphy, Upper Pennsylvanian and Lower Permian Strata, North- and West-Central Texas: Texas Bureau of Economic Geology, Report of Investigations 197, 116 p.

BRYANT, M., FALK, P., AND PAOLA, C., 1995, Experimental study of avulsion frequency and rate of deposition: *Geology*, v. 23, p. 365–368.

CATUNEANU, O., 2006, *Principles of Sequence Stratigraphy*: Amsterdam, Elsevier, 375 p.

CHARVIN, K., HAMPSON, G.J., GALLAGHER, K.L., AND LABOURDETTE, R., 2010, Intra-parasequence architecture of an interpreted asymmetrical wave-dominated delta: *Sedimentology*, v. 57, p. 760–785.

CHUMAKOV, N.M., ZHARKOV, M.A., HERMAN, A.B., DOLUDENKO, M.P., KALANDADZE, N.N., LEBEDEV, E.L., AND RAUTIAN, A.S., 1995, Climatic belts of the mid-Cretaceous time: *Stratigraphy and Geological Correlation*, v. 3, p. 42–63.

CLIFTON, H.E., HUNTER, R.E., AND PHILLIPS, R.L., 1971, Depositional structures and processes in the non-barred high-energy nearshore: *Journal of Sedimentary Petrology*, v. 41, p. 651–670.

COATES, L., AND MACÉACHERN, J.A., 2009, The ichnological signatures of river- and wave-dominated delta complexes: differentiating deltaic and non-deltaic shallow marine successions, Lower Cretaceous Viking Formation and Upper Cretaceous Dunvegan Formation, west-central Alberta, in MacEachern, J.A., Bann, K.L., Gingras, M.K., and Pemberton, S.G., eds., *Applied Ichnology: SEPM, Short Course Notes 52*, p. 227–254.

DAVIDSON, S.K., HARTLEY, A.J., WEISSMANN, G.S., NICHOLS, G.J., AND SCUDERI, L.A., 2013, Geomorphic elements on modern distributive fluvial systems: *Geomorphology*, v. 180, p. 82–95.

DECELLES, P.G., 2004, Late Jurassic to Eocene evolution of the Cordilleran thrust belt and foreland basin system, western U.S.A.: *American Journal of Science*, v. 304, p. 105–168.

DI CELMA, C., RAGAINI, L., AND CAFFAU, M., 2016, Marine and nonmarine deposition in a long-term low-accommodation setting: an example from the middle Pleistocene Qm2 unit, eastern central Italy: *Marine and Petroleum Geology*, v. 72, p. 234–253.

DOLLIVER, P.N., 1985, The Plio-Pleistocene Canadian breaks of New Mexico: a profile: *New Mexico Geological Society, 36th Annual Field Conference, Guidebook*, p. 315–318.

EDMONDS, D.A., AND SLINGERLAND, R.L., 2007, Mechanics of river mouth bar formation: implications for the morphodynamics of delta distributary networks: *Journal of Geophysical Research*, v. 112, no. F02034.

- ELDRITT, J.S., MA, C., BERGMAN, S.C., OZKAN, A., MINISINI, D., LUTZ, B., JACKETT, S.J., MACAULAY, C., AND KELLY, A.E., 2015, Origin of limestone–marlstone cycles: astronomic forcing of organic-rich sedimentary rocks from the Cenomanian to early Coniacian of the Cretaceous Western Interior Seaway, USA: *Earth and Planetary Science Letters*, v. 423, p. 98–113.
- EMBRY, A.F., 2002, Transgressive–regressive (T-R) sequence stratigraphy: Gulf Coast Association of Geological Societies, *Transactions*, v. 52, p. 151–172.
- EMERY, D., AND MYERS, K., 2009, *Sequence Stratigraphy*: New York, John Wiley & Sons, p. 297.
- ENGE, H.D., HOWELL, J.A., AND BUCKLEY, S.J., 2010, Quantifying clinothem geometry in a forced-regressive river-dominated delta, Panther Tongue, Utah, USA: *Sedimentology*, v. 57, p. 1750–1770.
- FABUEL-PEREZ, I., HODGETTS, D., AND REDFERN, J., 2009, A new approach for outcrop characterization and geostatistical analysis of a low-sinuosity fluvial-dominated succession using digital outcrop models: Upper Triassic Oukaimeden Sandstone Formation, central High Atlas, Morocco: *American Association of Petroleum Geologists, Bulletin*, v. 93, p. 795–827.
- FAN, D., YUAN, W., AND MIN, L., 2013, Classifications, sedimentary features and facies associations of tidal flats: *Journal of Palaeogeography*, v. 2, p. 66–80.
- FIDOLINI, F., AND GHINASSI, M., 2016, Friction- and inertia-dominated effluents in a lacustrine, river-dominated deltaic succession (Pliocene upper Valdarno Basin, Italy): *Journal of Sedimentary Research*, v. 86, p. 1083–1101. doi:10.2110/jsr.2016.65
- FIELDING, C.R., 2008, Sedimentology and stratigraphy of large river deposits: recognition in the ancient record, and distinction from “Incised Valley Fills,” in Gupta, A., eds., *Large Rivers: Geomorphology and Managements*: John Wiley & Sons, p. 97–113.
- FIELDING, C.R., TRUEMAN, J.D., AND ALEXANDER, J., 2005, Sharp-based, flood-dominated mouth bar sands from the Burdekin River Delta of northeastern Australia: extending the spectrum of mouth-bar facies, geometry, and stacking patterns: *Journal of Sedimentary Research*, v. 75, p. 55–66.
- FIELDING, C.R., TRUEMAN, J.D., AND ALEXANDER, J., 2006, Holocene depositional history of the Burdekin River Delta of northeastern Australia: a model for a low-accommodation, highstand delta: *Journal of Sedimentary Research*, v. 76, p. 411–28.
- FIELDING, C.R., BANN, K.L., AND TRUEMAN, J.D., 2009, Resolving the architecture of a complex, low-accommodation unit using high-resolution sequence stratigraphy and ichnology: the Late Permian Freitag Formation in the Denison Trough, Queensland, Australia: *SEPM, Short Course Notes* 52, p. 1–30.
- FLEMMING, B.W., 2000, The role of grain size, water depth and flow velocity as scaling factors controlling the size of subaqueous dunes: *Marine Sandwave Dynamics, International Workshop, Proceedings*, p. 55–60.
- FRIEND, P.F., SLATER, M.J., AND WILLIAMS, R.C., 1979, Vertical and lateral building of river sandstone bodies, Ebro Basin, Spain: *Geological Society of London, Journal*, v. 136, p. 39–46.
- GALLOWAY, W.E., 1975, Process framework for describing the morphologic and stratigraphic evolution of deltaic depositional systems, in Broussard, M.L., eds., *Deltas: Models for Exploration*: Houston Geological Society, p. 87–98.
- GALLOWAY, W.E., 1989, Genetic stratigraphic sequences in basin analysis I: architecture and genesis of flooding-surface bounded depositional units: *American Association of Petroleum Geologists, Bulletin*, v. 73, p. 125–142.
- GANI, M.R., AND BHATTACHARYA, J.P., 2005, Lithostratigraphy versus chronostratigraphy in facies correlations of Quaternary deltas: application of bedding correlation, in Giosan, L., and Bhattacharya, J.P., eds., *River Deltas, Concepts, Models, and Examples*: SEPM, Special Publication 83, p. 31–48.
- GANI, M.R., AND BHATTACHARYA, J.P., 2007, Basic building blocks and process variability of a Cretaceous delta: internal facies architecture reveals a more dynamic interaction of river, wave, and tidal processes than is indicated by external shape: *Journal of Sedimentary Research*, v. 77, p. 284–302.
- GANI, M.R., BHATTACHARYA, J.P., AND MACEachern, J.A., 2009, Using ichnology to determine the relative influence of waves, storms, tides, and rivers in deltaic deposits: examples from Cretaceous Western Interior Seaway, U.S.A.: *applied ichnology*: SEPM, Short Course Notes 52, p. 209–255.
- GARRISON, J.R., JR., AND VAN DEN BERGH, T.C.V., 2004, The high-resolution depositional sequence stratigraphy of the Upper Ferron sandstone Last Chance Delta: an application of coal-zone stratigraphy, in Chidsey, T.C., Jr., Adams, R.D., and Morrison, T.H., eds., *Analog for Fluvial–Deltaic Reservoir Modeling*: Ferron Sandstone of Utah: American Association of Petroleum Geologists, *Studies in Geology*, v. 50, p. 125–92.
- GELEYNSE, N., STORMS, J.E.A., WALSTRA, D.J.R., JAGERS, H.R.A., WANG, Z.B., AND STIVE, M.J.F., 2011, Controls on river delta formation: insights from numerical modeling: *Earth and Planetary Science Letters*, v. 302, p. 217–26.
- HAMPSON, G.J., 2016, Towards a sequence stratigraphic solution set for autogenic processes and allogenic controls: Upper Cretaceous strata, Book Cliffs, Utah, USA: *Geological Society of London, Journal*, v. 173, p. 817–36.
- HELLAND-HANSEN, W., AND GJELBERG, J.G., 1994, Conceptual basis and variability in sequence stratigraphy: a different perspective: *Sedimentary Geology*, v. 92, p. 31–52.
- HELLAND-HANSEN, W., AND MARTINSEN, O.J., 1996, Shoreline trajectories and sequences: description of variable depositional-dip scenarios: *Journal of Sedimentary Research*, v. 66, p. 670–88.
- HOLBROOK, J.M., 1996, Complex fluvial response to low gradients at maximum regression: a genetic link between smooth sequence-boundary morphology and architecture of overlying sheet sandstone: *Journal of Sedimentary Research*, v. 66, p. 713–22.
- HOLBROOK, J., 2001, Origin, genetic interrelationships, and stratigraphy over the continuum of fluvial channel-form bounding surfaces: an illustration from middle Cretaceous strata, southeastern Colorado: *Sedimentary Geology*, v. 144, p. 179–222.
- HOLBROOK, J.M., AND BHATTACHARYA, J.P., 2012, Reappraisal of the sequence boundary in time and space: case and considerations for an SU (subaerial unconformity) that is not a sediment bypass surface, a time barrier, or an unconformity: *Earth-Science Reviews*, v. 113, p. 271–302.
- HOLBROOK, J.M., AND DUNBAR, R.W., 1992, Depositional history of Lower Cretaceous strata in northeastern New Mexico: implications for regional tectonics and depositional sequences: *Geological Society of America, Bulletin*, v. 104, p. 802–813.
- HOLBROOK, J.M., AND WHITE, D.C., 1998, Evidence for subtle uplift from lithofacies distribution and sequence architecture: examples from lower Cretaceous strata of northeastern New Mexico, in Shanley, K.W., and McCabe, P.J., eds., *Relative Role of Eustasy, Climate, and Tectonism in Continental Rocks*: SEPM, Special Publication 59, p. 123–132.
- HOLBROOK, J.M., SCOTT, R.W., AND OBOH-IKUENOBE, F.E., 2006, Base-level buffers and buttresses: a model for upstream versus downstream control on fluvial geometry and architecture within sequences: *Journal of Sedimentary Research*, v. 76, p. 162–74.
- JEROLMACK, D.J., AND MOHRIG, D., 2007, Conditions for branching in depositional rivers: *Geology*, v. 35, p. 463.
- JEROLMACK, D.J., AND SWENSON, J.B., 2007, Scaling relationships and evolution of distributary networks on wave-influenced deltas: *Geophysical Research Letters*, v. 34, no. L23402.
- KISUCKY, M.J., 1987, *Sedimentology, Stratigraphy and Paleogeography of the Lower Cretaceous Mesa Rica Delta System, Tucumcari Basin, East-Central New Mexico* [MS Thesis]: University of New Mexico, Albuquerque, 124 p.
- KISUCKY, M.J., AND WRIGHT, R., 1986, Facies relationships in Mesa Rica Sandstone (Lower Cretaceous), Tucumcari Basin, east-central New Mexico: *American Association of Petroleum Geologists, Bulletin*, v. 70, p. 345–346.
- KUES, B.S., AND LUCAS, S.G., 2001, Nearshore fauna of the Tucumcari Formation (Lower Cretaceous, Albian): *New Mexico Geological Society, 52nd Annual Field Conference, Guidebook*, p. 229–249.
- LI, W., BHATTACHARYA, J.P., ZHU, Y., GARZA, D., AND BLANKENSHIP, E., 2011, Evaluating delta asymmetry using three-dimensional facies architecture and ichnological analysis, Ferron “Notom Delta,” Capital Reef, Utah, USA: *Sedimentology*, v. 58, p. 478–507.
- LIANG, M., VOLLER, V.R., AND PAOLA, C., 2015, A reduced-complexity model for river delta formation, Part I: modeling deltas with channel dynamics: *Earth Surface Dynamics*, v. 3, p. 67–86.
- LUCAS, S.G., AND KISUCKY, J., 1988, Type and reference sections of the Tucumcari, Mesa Rica, and Pajarito formations, Cretaceous of east-central New Mexico: *New Mexico Geology*, v. 10, p. 82–89.
- MA, C., MEYERS, S.R., SAGEMAN, B.B., SINGER, B.S., AND JICHA, B.R., 2014, Testing the astronomical time scale for Oceanic Anoxic Event 2, and its extension into Cenomanian strata of the Western Interior Basin (USA): *Geological Society of America, Bulletin*, v. 126, p. 974–989.
- MACEachern, J.A., AND BANN, K.L., 2008, The role of ichnology in refining shallow marine facies models, in Hampson, G.J., Steel, R.J., Burgess, P.M., and Dalrymple, R.W., eds., *Recent Advances in Models of Siliciclastic Shallow-Marine Stratigraphy*, v. 90, p. 73–116.
- MACEachern, J.A., BANN, K.L., BHATTACHARYA, J.P., AND HOWELL, C.D., 2005, Ichnology of deltas, in Giosan, L., and Bhattacharya, J.P., eds., *River Deltas, Concepts, Models, and Examples*: SEPM, Special Publication 83, p. 49–85.
- MACKENZIE, D.B., AND POOLE, D.M., 1962, Provenance of Dakota Group Sandstones of the Western Interior: *Wyoming Geological Association, 17th Field Conference*, p. 62–71.
- MADOFF, A.S., HARRIS, A.D., AND CONNELL, S.D., 2016, Nearshore along-strike variability: Is the concept of the systems tract unhelped? *Geology*, v. 44, p. 315–318.
- MARTIN, J., CANTELLI, A., PAOLA, C., BLUM, M., AND WOLINSKY, M., 2011, Quantitative modeling of the evolution and geometry of incised valleys: *Journal of Sedimentary Research*, v. 81, p. 64–79.
- MARTINSEN, O.J., 1993, Namurian (Late Carboniferous) depositional systems of the Craven–Askrigg area, northern England: implications for sequence-stratigraphic models, in Posamentier, H.W., Summerhayes, C.P., Haq, B.U., and Allen, P., eds., *Sequence Stratigraphy and Facies Associations*: International Association of Sedimentologists, Special Publication 18, p. 247–281.
- MARTINSEN, O.J., AND HELLAND-HANSEN, W., 1995, Strike variability of clastic depositional systems: Does it matter for sequence-stratigraphic analysis? *Geology*, v. 23, p. 439–442.
- MIALL, A.D., 1985, Architectural-element analysis: a new method of facies analysis applied to fluvial deposits: *Earth-Science Reviews*, v. 22, p. 261–308.
- MIALL, A.D., 1988, Reservoir heterogeneities in fluvial sandstones: lessons from outcrop studies: *American Association of Petroleum Geologists, Bulletin*, v. 72, p. 682–97.
- MIALL, A.D., 2014, *Fluvial Depositional Systems*: Berlin, Springer International Publishing, p. 316.
- MILLER, K.G., SUGARMAN, P.J., BROWNING, J.V., KOMINZ, M.A., OLSSON, R.K., FEIGENSON, M.D., AND HERNÁNDEZ, J.C., 2004, Upper Cretaceous sequences and sea-level history, New Jersey Coastal Plain: *Geological Society of America, Bulletin*, v. 116, p. 368–393.
- MULDER, T., SVYITSKI, J.P.M., MIGEON, S., FAUGÈRES, J.C., AND SAVOYE, B., 2003, Marine hyperpycnal flows: initiation, behavior, and related deposits. a review: *Marine and Petroleum Geology*, v. 20, p. 861–882.

- MUTO, T., AND STEEL, R.J., 1997, Principles of regression and transgression: the nature of the interplay between accommodation and sediment supply: *Journal of Sedimentary Research*, v. 67, p. 994–1000.
- MUTO, T., AND STEEL, R.J., 2004, Autogenic response of fluvial deltas to steady sea-level fall: implications from flume-tank experiments: *Geology*, v. 32, p. 401–404.
- MUTO, T., FURUBAYASHI, R., TOMER, A., SATO, T., KIM, W., NARUSE, H., AND PARKER, G., 2016, Planform evolution of deltas with graded alluvial topsets: insights from three-dimensional tank experiments, geometric considerations and field applications: *Sedimentology*, v. 63, p. 2158–2189.
- NEAL, J., AND ABREU, V., 2009, Sequence stratigraphy hierarchy and the accommodation succession method: *Geology*, v. 37, p. 779–782.
- NORMARK, W.R., POSAMANTIER, H., AND MUTTI, E., 1993, Turbidite systems: state of the art and future directions: *Reviews of Geophysics*, v. 31, p. 91–116.
- OBOH-IKUENOBE, F.E., HOLBROOK, J.M., SCOTT, R.W., AKINS, S.L., EVETTS, M.J., BENSON, D.G., AND PRATT, L.M., 2008, Anatomy of epicontinental flooding: late Albian–early Cenomanian of the southern U.S. Western Interior Basin, in Pratt, B.R., and Holmden, C., eds., *Dynamics of Epeiric Seas: Geological Association of Canada, Special Paper 48*, p. 201–227.
- OLARIU, C., 2014, Autogenic process change in modern deltas: lessons for the ancient, in Martinius, A.W., Ravnås, R., Howell, J.A., Steel, R.J., and Wonham, J.P., eds., *From Depositional Systems to Sedimentary Successions on the Norwegian Continental Margin: International Association of Sedimentologists, Special Publication 47*, p. 149–166.
- OLARIU, C., AND BHATTACHARYA, J.P., 2006, Terminal distributary channels and delta front architecture of river-dominated delta systems: *Journal of Sedimentary Research*, v. 76, p. 212–233.
- OLARIU, C., BHATTACHARYA, J.P., XU, X., AIKEN, C.L.V., ZENG, X., AND MCMEEHAN, G.A., 2005, Integrated study of ancient delta-front deposits, using outcrop, ground penetrating radar, and three dimension photorealistic data: *Cretaceous Panther Tongue sandstone, Utah*, in Giosan, L., and Bhattacharya, J.P., eds., *River Deltas, Concepts, Models, and Examples: SEPM, Special Publication 83*, p. 155–178.
- OLARIU, C., STEEL, R.J., AND PETTER, A.L., 2010, Delta-front hyperpycnal bed geometry and implications for reservoir modeling: *Cretaceous Panther Tongue delta, Book Cliffs, Utah: American Association of Petroleum Geologists, Bulletin*, v. 94, p. 819–845.
- ORTON, G.J., AND READING, H.G., 1993, Variability of deltaic processes in terms of sediment supply, with particular emphasis on grain size: *Sedimentology*, v. 40, p. 475–512.
- OVEREEM, I., KROONENBERG, S.B., VELDKAMP, A., GROENESTEIJN, K., RUSAKOV, G.V., AND SVITICH, A.A., 2003, Small-scale stratigraphy in a large ramp delta: recent and Holocene sedimentation in the Volga delta, Caspian Sea: *Sedimentary Geology*, v. 159, p. 133–57.
- PAOLA, C., AND MOHRIG, D., 1996, Palaeohydraulics revisited: palaeoslope estimation in coarse-grained braided rivers: *Basin Research*, v. 8, p. 243–254.
- PATRUÑO, S., HAMPSON, G.J., AND JACKSON, C.A.L., 2015, Quantitative characterisation of deltaic and subaqueous clinofolds: *Earth-Science Reviews*, v. 142, p. 79–119.
- PATTISON, S.A.J., 2018, Rethinking the incised-valley fill paradigm for Campanian Book Cliffs strata, Utah–Colorado, U.S.A.: evidence for discrete parasequence-scale, shoreface-incised channel fills: *Journal of Sedimentary Research*, v. 88, p. 1381–1412. doi:10.2110/jsr.2018.72
- PLINT, A.G., 2000, Sequence stratigraphy and paleogeography of a Cenomanian deltaic complex: the Dunvegan and Lower Kaskapau formations in subsurface and outcrop, Alberta and British Columbia, Canada: *Bulletin of Canadian Petroleum Geology*, v. 48, p. 43–79.
- POSAMANTIER, H.W., AND MORRIS, W.R., 2000, Aspects of the stratal architecture of forced regressive deposits, in Hunt, D., and Gawthorpe, R.L., eds., *Sedimentary Response to Forced Regressions: Geological Society of London, Special Publication 172*, p. 19–46.
- POSAMANTIER, H.W., AND VAIL, P.R., 1988, Eustatic controls on clastic deposition II: sequence and systems tract models, in Wilgus, C.K., Hastings, B.S., Kendall, C.G.St.C., Posamentier, H.W., Ross, C.A., and Van Wagoner, J.S., eds., *Sea-Level Changes: An Integrated Approach: SEPM, Special Publication 42*, p. 125–154.
- POSAMANTIER, H.W., JERVEY, M.T., AND VAIL, P.R., 1988, Eustatic controls on clastic deposition I: conceptual framework, in Wilgus, C.K., Hastings, B.S., Kendall, C.G.St.C., Posamentier, H.W., Ross, C.A., and Van Wagoner, J.S., eds., *Sea-Level Changes: An Integrated Approach: SEPM, Special Publication 42*, p. 110–124.
- POSTMA, G., 1990, An analysis of the variation in delta architecture: *Terra Nova*, v. 2, p. 124–130.
- POTTER, P.E., 1967, Sand bodies and sedimentary environments: a review: *American Association of Petroleum Geologists, Bulletin*, v. 51, p. 337–365.
- SCOTT, R.W., 1970, Stratigraphy and sedimentary environments of Lower Cretaceous rocks, southern Western Interior: *American Association of Petroleum Geologists, Bulletin*, v. 54, p. 1225–1244.
- SCOTT, R.W., 1974, Bay and shoreface benthic communities in the Lower Cretaceous: *Lethaia*, v. 7, p. 315–330.
- SCOTT, R.W., FRANKS, P.C., EVETTS, M.J., BERGEN, J.A., AND STEIN, J.A., 1998, Timing of mid-Cretaceous relative sea-level changes in the Western Interior: Amoco No. 1 bounds core, in Dean, W.E., and Arthur, M.A., eds., *Stratigraphy and Palaeoenvironments of the Cretaceous Western Interior Seaway, USA: SEPM, Concepts in Sedimentology and Paleontology 6*, p. 11–34.
- SCOTT, R.W., HOLBROOK, J.M., OBOH-IKUENOBE, F.E., EVETTS, M.J., BENSON, D.G., AND KUES, B.S., 2004, Middle Cretaceous stratigraphy, southern Western Interior Seaway, New Mexico and Oklahoma: *The Mountain Geologist*, v. 41, p. 33–59.
- SCOTT, R.W., OBOH-IKUENOBE, F.E., BENSON, D.G., HOLBROOK, J.M., AND ALNAHWI, A., 2018, Cenomanian–Turonian flooding cycles: U.S. Gulf Coast and Western Interior: *Cretaceous Research*, v. 89, p. 191–210.
- SLINGERLAND, R., AND SMITH, N.D., 2004, River Avulsions and their deposits: *Annual Review of Earth and Planetary Sciences*, v. 32, p. 257–285.
- STEARNS, D.W., 1972, Structural interpretation of the fractures associated with the Bonita fault: *New Mexico Geological Society, 23rd Annual Field Conference, Guidebook*, p. 161–64.
- STORMS, J.E., STIVE, M.J., ROELVINK, D.J.A., AND WALSTRA, D.J., 2007, Initial morphologic and stratigraphic delta evolution related to buoyant river plumes, in *Coastal Sediments: New Orleans, America Society of Civil Engineers*, v. 7, p. 736–748.
- STRONG, N., AND PAOLA, C., 2008, Valleys that never were: time surfaces versus stratigraphic surfaces: *Journal of Sedimentary Research*, v. 78, p. 579–593.
- SULEIMAN, A.S., AND KELLER, G.R., 1985, A Geophysical Study of Basement Structure in Northeastern New Mexico: *New Mexico Geological Society, 36th Annual Field Conference, Guidebook*, p. 153–159.
- TALLING, P.J., 1998, How and where do incised valleys form if sea level remains above the shelf edge?: *Geology*, v. 26, p. 87–90.
- TAYLOR, A.M., AND GOLDRING, R., 1993, Description and analysis of bioturbation and ichnofabric: *Geological Society of London, Journal*, v. 150, p. 141–148.
- VAKARELOV, B.K., BHATTACHARYA, J.P., AND NEBRIGIC, D.D., 2006, Importance of high-frequency tectonic sequences during greenhouse times of Earth history: *Geology*, v. 34, p. 797–800.
- VAN WAGONER, J.C., POSAMANTIER, H.W., MITCHUM, R.M., VAIL, P.R., SARG, J.F., LOUITT, T.S., AND HARDENBOL, J., 1988, An overview of the fundamentals of sequence stratigraphy and key definitions, in Wilgus, C.K., Hastings, B.S., Kendall, C.G.St.C., Posamentier, H.W., Ross, C.A., and Van Wagoner, J.C., eds., *Sea-Level Changes: An Integrated Approach: SEPM, Special Publication 42*, p. 39–45.
- WALKER, R.G., AND BERGMAN, K.M., 1993, Shannon Sandstone in Wyoming: a shelf-ridge complex reinterpreted as lowstand shoreface deposits: *Journal of Sedimentary Petrology*, v. 63, p. 839–851.
- WILLIS, B.J., BHATTACHARYA, J.P., GABEL, S.L., AND WHITE, C.D., 1999, Architecture of a tide-influenced river delta in the Frontier Formation of central Wyoming, USA: *Sedimentology*, v. 46, p. 667–688.
- WINN, R.D., 1991, Storm deposition in marine sand sheets: Wall Creek Member, Frontier Formation, Powder River Basin, Wyoming: *Journal of Sedimentary Petrology*, v. 61, p. 86–101.
- WRIGHT, L.D., AND COLEMAN, J.M., 1973, Variations in morphology of major river deltas as functions of ocean wave and river discharge regimes: *American Association of Petroleum Geologists, Bulletin*, v. 57, p. 370–398.
- ZAITLIN, B.A., DALRYMPLE, R.W., AND BOYD, R., 1994, The stratigraphic organization of incised valley systems associated with relative sea-level change, in Dalrymple, R.W., Boyd, R., and Zaitlin, B.A., eds., *Incised-Valley Systems: Origin and Sedimentary Sequences: SEPM, Special Publication 51*, p. 45–60.
- ZAVALA, C., AND ARCURI, M., 2016, Intrabasinal and extrabasinal turbidites: origin and distinctive characteristics: *Sedimentary Geology*, v. 337, p. 36–54.

Received 9 July 2018; accepted 11 March 2019.